



1 Effect of soil saturation on denitrification in a grassland soil

2 Laura Maritza Cardenas^{1*}, Roland Bol, R.², Dominika Lewicka-Szczebak,³, Andrew Stuart
3 Gregory⁴, Graham Peter Matthews⁵, William Richard Whalley⁴, Thomas Henry Misselbrook¹,
4 David Scholefield¹ and Reinhard Well³

5

6 ¹Rothamsted Research, North Wyke, Okehampton, Devon EX20 2SB, United Kingdom

7 ²Institute of Bio- and Geosciences, IBG-3/Agrosphere, Forschungszentrum Jülich GmbH, 52428
8 Jülich, Germany

9 ³Thünen Institute of Climate-Smart Agriculture, Federal Research Institute for Rural Areas,
10 Forestry and Fisheries, Bundesallee, 50, D-38116 Braunschweig, Germany

11 ⁴Rothamsted Research, Harpenden, Hertfordshire AL5 2JQ, United Kingdom

12 ⁵University of Plymouth, Drake Circus, Plymouth, Devon PL4 8AA, United Kingdom

13 *Correspondence to: Laura M. Cardenas (laura.cardenas@rothamsted.ac.uk)

14

15 **Abstract.** Nitrous oxide (N₂O) is of major importance as a greenhouse gas and precursor of
16 ozone (O₃) destruction in the stratosphere mostly produced in soils. The soil emitted N₂O is
17 predominantly derived from denitrification and to a smaller extent, nitrification in soils, both
18 processes controlled by environmental factors and their interactions, and are influenced by
19 agricultural management. Soil water content expressed as water filled pore space (WFPS) is a major
20 controlling factor of emissions and its interaction with compaction, has not been studied at the
21 micropore scale. A laboratory incubation was carried out at different saturation levels for a
22 grassland soil and emissions of N₂O and N₂ were measured as well as the isotopomers of N₂O. We
23 found that fluxes variability was larger in the less saturated soils probably due to nutrient
24 distribution heterogeneity created from soil cracks and consequently nutrient hot spots. The results
25 agreed with denitrification as the main source of fluxes at the highest saturations, but nitrification
26 could have occurred at the lower saturation, even though moisture was still high (71% WFPS). The
27 isotopomer data showed isotopic similarities in the wettest treatments vs the two drier ones; and



28 results agreed with previous findings where it is clear there are 2 N-pools with different dynamics:
29 added N producing intense denitrification, vs soil N resulting in less isotopic fractionation.

30 **Keywords**

31 Grassland, nitrous oxide, isotopomers, isotopologues, greenhouse gases
32

33 **1 Introduction**

34 Nitrous oxide (N_2O) is of major importance as a greenhouse gas and precursor of ozone (O_3)
35 destruction in the stratosphere (Crutzen, 1970). Agriculture is a major source of greenhouse gases
36 (GHGs), such as carbon dioxide (CO_2), methane (CH_4) and also N_2O (IPCC, 2006). The application
37 of organic and inorganic fertiliser N to agricultural soils enhances the production of N_2O (Baggs *et*
38 *al.*, 2000). This soil emitted N_2O is predominantly derived from denitrification and to a smaller extent,
39 nitrification in soils (Davidson and Verchot, 2000). Denitrification is a microbial process in which
40 reduction of nitrate (NO_3^-) occurs to produce N_2O , and N_2 is the final product of this process, benign
41 for the environment, but represents a loss of N in agricultural systems. Nitrification is an oxidative
42 process in which ammonium (NH_4^+) is converted to NO_3^- (Davidson and Verchot, 2000). Both
43 processes are controlled by environmental factors and their interactions, and are influenced by
44 agricultural management (Firestone and Davidson, 1989). It is well recognised that soil water content
45 expressed as water filled pore space (WFPS) is a major controlling factor and as Davidson (1991)
46 illustrated, nitrification is a source of N_2O until WFPS values reach about 70%, after which
47 denitrification dominates. In fact, Firestone and Davidson (1989) gave oxygen supply a ranking of 1
48 in importance as a controlling factor in fertilised soils, above C and N. At WFPS between 45 and
49 75% a mixture of nitrification and denitrification act as N_2O sources. Davidson also suggested that at
50 WFPS values above 90% only N_2 is produced. Several studies have later proposed models to relate
51 WFPS with emissions (Schmidt *et al.*, 2000; Dobbie and Smith, 2001; Parton *et al.*, 2001; del Prado
52 *et al.*, 2006; Castellano *et al.*, 2010) but the “optimum” WFPS for N_2O emissions varies from soil to
53 soil (Davidson, 1991). Soil structure could be influencing this effect and it has been identified to
54 strongly interact with soil moisture (Ball *et al.*, 1999; van Groenigen *et al.*, 2005) through changes in



55 WFPS. Particularly soil compaction due to livestock treading and the use of heavy machinery affect
56 soil structure and emissions as shown by studies relating bulk density to fluxes (Kleftho *et al.*, 2014b);
57 and degrees of tillage to emissions (Ludwig *et al.*, 2011).

58 Compaction is known to affect the size of the larger pores (macropores) thereby reducing the
59 soil air volume and therefore increasing the WFPS (for the same moisture content) (van der Weerden
60 *et al.*, 2012). However, little is known about the effect of compaction on the smaller soil pores
61 (micropores) and this could provide valuable information for understanding the simultaneous
62 behaviour of the dynamics of water in the various pore sizes in soil. Such an understanding would
63 lead to the development of better N₂O mitigation strategies via dealing with soil compaction issues.

64 The role of water in soils is closely linked to microbial activity but also relates to the degree
65 of aeration and gas diffusivity in soils (Morley and Baggs, 2010). Water facilitates nutrient supply to
66 microbes and restricts gas diffusion, thereby increasing the residence time of gases in soil, and the
67 chance of further N₂O reduction before it can be released to the atmosphere. This is further aided by
68 the restriction of the diffusion of atmospheric O₂ (Dobbie and Smith, 2001), increasing the potential
69 for denitrification. As a consequence, counteracting effects (high microbial activity vs low diffusion)
70 occur simultaneously making it difficult to predict net processes and corresponding outputs
71 (Davidson, 1991). Detailed understanding of the sources of N₂O and the influence of physical factors,
72 i.e. soil structure and its interaction with moisture, is a powerful tool for developing effective
73 mitigation strategies.

74 Isotopologues of N₂O represent the isotopic substitution of the O and/or the two N atoms
75 within the N₂O molecule. The isotopomers of N₂O, are those differing in the peripheral (β) and central
76 N-positions (α) of the linear molecule (Toyoda and Yoshida, 1999) with the intramolecular ¹⁵N site
77 preference (SP; the difference between $\delta^{15}\text{N}^\alpha - \delta^{15}\text{N}^\beta$) used to identify production processes at the
78 level of microbial species or enzymes involved (Toyoda *et al.*, 2005; Ostrom, 2011). Moreover, $\delta^{18}\text{O}$,
79 $\delta^{15}\text{N}$ and SP of emitted N₂O depend on the denitrification product ratio (N₂O / (N₂+N₂O)), and hence
80 provide insight into the dynamics of N₂O reduction (Well and Flessa, 2009; Lewicka-Szczebak *et al.*,



81 2015; Lewicka-Szczebak *et al.*, 2014). Data reported in the literature provide values for these
82 parameters in relation to the source process for N₂O. Koster *et al.* (2013) for example recently
83 reported $\delta^{15}\text{N}^{\text{bulk}}$ values of N₂O between $-36.8\text{\textperthousand}$ and $-31.9\text{\textperthousand}$ in the conditions of their experiment,
84 which are indicative of denitrification according to Perez *et al.* (2006) and Well and Flessa (2009)
85 who proposed the range -54 to $-10\text{\textperthousand}$ relative to the substrate. Baggs (2008) summarised that values
86 between -90 to $-40\text{\textperthousand}$ are indicative of nitrification. Determination of these values are normally
87 carried out in pure culture studies or in conditions favouring either production or reduction of N₂O
88 (Well and Flessa, 2009). The SP is however considered a better predictor of the N₂O source due to
89 its independence from the substrate signature (Ostrom, 2011).

90 Simultaneous occurrence production and reduction of N₂O as in natural conditions presents
91 a challenge for isotopic factors determination due to uncertainty on N₂ reduction and the co-existence
92 of different microbial communities resulting in other steps of denitrification happening as well
93 (Lewicka-Szczebak *et al.*, 2014). Recently, using data from the experiment here reported, where soil
94 was incubated under aerobic atmosphere and the complete denitrification process occurs, Lewicka-
95 Szczebak *et al.* (2015) determined fractionation factors associated with N₂O production and reduction
96 using a modelling approach. The analysis comprised measurements of the N₂O and N₂ fluxes
97 combined with isotopomer data. The results generally confirmed the range of values of η (net isotope
98 effects) and $\eta^{18}\text{O}/\eta^{15}\text{N}$ ratios reported by previous studies for N₂O reduction for the soil volume
99 reached by the N+C amendment. This did not apply for the soil volume not reached by the N+C
100 amendment.

101 Lewicka-Szczebak *et al.* (2015) observed a clear relationship between ^{15}N and ^{18}O isotope
102 effects during N₂O production and denitrification rates. For N₂O reduction, differential isotope effects
103 were observed for two distinct soil pools characterized by different product ratios N₂O / (N₂+N₂O).
104 For moderate product ratios (from 0.1 to 1.0) the range of isotope effects given by previous studies
105 was confirmed and refined, whereas for very low product ratios (below 0.1) the net isotope effects
106 were much smaller. In this paper, we present the results from the gas emissions measurements from



107 soils collected from a long-term permanent grassland soil to assess the impact of different levels of
108 soil saturation on N_2O and N_2 and CO_2 emissions after compaction. The measurements included the
109 soil isotopomer ($^{15}\text{N}_a$, $^{15}\text{N}_\beta$ and site preference) analysis of emitted N_2O , which in combination with
110 the bulk ^{15}N and ^{18}O was used to distinguish between N_2O from bacterial denitrification and other
111 processes (e.g. nitrification and fungal denitrification) (Lewicka-Szczebak, 2016a).

112 The study was carried out under laboratory controlled conditions, using a specialised
113 laboratory denitrification (DENIS) incubation system (Cardenas *et al.*, 2003). The system allows
114 continuous measurements of N gases as well as CO_2 , and spot sampling for isotopomer analyses.

115 We conducted measurements at defined saturation of pores size fractions as a prerequisite to
116 model denitrification as a function of water status (Butterbach Bahl *et al.*, 2013 and Müller and
117 Clough, 2014). We have under controlled conditions created a single compaction stress of 200 kPa
118 in incremental layers using a uniaxial pneumatic piston to simulate a grazing pressure. We
119 hypothesized that at high water saturation, heterogeneity in N emissions decreases due to more
120 homogeneous distribution of the soil nutrients and/or anaerobic microsites. We also hypothesized that
121 even at high soil moisture a mixture of nitrification and denitrification can occur. We aimed to
122 understand changes in the ratio $\text{N}_2\text{O}/(\text{N}_2\text{O}+\text{N}_2)$ and the behaviour and utility of isotopologues of N_2O
123 at the different moisture levels studied in a controlled manner on soil micro and macropores.

124 **2 Materials and methods**

125 **2.1 Soil used in the study**

126 An agricultural soil, under grassland management since at least 1838 (Barré *et al.*, 2010), was
127 collected from a location adjacent to a long-term ley-arable experiment at Rothamsted Research in
128 Hertfordshire (Highfield, see soil properties in Table 1 and further details in Rothamsted Research,
129 2006; Gregory *et al.*, 2010). The soil had been under permanent cut mixed-species (predominantly
130 *Lolium* and *Trifolium*) vegetation. The soil was sampled as described in Gregory *et al.* (2010). Briefly
131 it was sampled from the upper 150 mm of the profile, air dried in the laboratory, crumbled and sieved



132 (<4 mm), mixed to make a bulk sample and equilibrated at a pre-determined water content (37 g 100
133 g⁻¹; Gregory *et al.*, 2010) in air-tight containers at 4° C for at least 48 hours.

134 **1.2.Preparation of soil blocks**

135 The equilibrated soil was then packed into twelve stainless steel blocks (145 mm diameter; h: 100
136 mm), each of which contained three cylindrical holes (i.d: 50 mm; h: 100 mm each), to a single
137 compaction stress of 200 kPa in incremental layers using a uniaxial pneumatic piston. The three hole-
138 blocks were used to facilitate the compression of the cores. The 200 kPa stress was analogous to a
139 severe compaction event by a tractor (Gregory *et al.*, 2010) or livestock (Scholefield *et al.*, 1985).
140 The total area of the upper surface of soil in each block was therefore 58.9 cm² (3 × 19.6 cm²) and
141 the target volume of soil was set to be 544.28 cm³ (3 × 181.43 cm³) with the objective of leaving a
142 headspace of approximately 45 cm³ (3 × 15 cm³) for the subsequent experiment. The precise height
143 of the soil (and hence the volume) was measured using the displacement measurement system of a
144 DN10 Test Frame (Davenport-Nene, Wigston, Leicester, UK) with a precision of 0.001 mm.

145 **2.3 Equilibration of soil cores at different saturations**

146 The soil was equilibrated to four different initial saturation conditions or treatments (t0) which were
147 based on the likely distribution of water between macropores and micropores. The first treatment was
148 where both the macro- and micropores (and hence the total soil) was fully saturated; the second
149 treatment was where the macropores were half-saturated and the micropores remained fully saturated;
150 the third treatment was where the macropores were fully unsaturated and the micropores again
151 remained fully saturated; and the fourth treatment was where the macropores were fully unsaturated
152 and the micropores were half-saturated. These four treatments are hereafter referred to as SAT/sat;
153 HALFSAT/sat; UNSAT/sat and UNSAT/halfsat, respectively, where upper-case refers to the
154 saturation condition of the macropores and lower-case refers to the saturation condition of the
155 micropores. In order to set these initial saturation conditions, we referred to the gravimetric soil water
156 release characteristic for the soil, as given in Gregory *et al.* (2010), which represents the assumed



157 pore size distribution, and a fitted van Genuchten function (van Genuchten, 1980) with the Mualem
158 (1976) constraint of $m = 1 - 1/n$:

$$159 \quad \theta_h = \theta_r + \frac{\theta_s - \theta_r}{[1 + (\alpha h)^n]^{1 - \frac{1}{n}}} \quad [1]$$

160

161 where θ_s , θ_r and θ_h are the saturated, residual (water content at permanent wilting point) and
162 h matric potential gravimetric water contents (g g^{-1}), respectively; h is the matric potential ($|\text{kPa}|$, i.e.
163 the absolute value), α is a fitted parameter approximating the inverse of h at the inflection point ($|\text{kPa}|^{-1}$,
164 often linked to the air-entry point, and m and n are dimensionless fitted parameters related to the
165 shape of the function.

166 The somewhat arbitrary saturation state known as “field capacity” represents the idealised
167 condition UNSAT/sat, where the macropores have drained and the micropores have yet to drain. As
168 field capacity has typically corresponded to a matric potential anywhere between -5 to -33 kPa, we
169 chose -20 kPa as our UNSAT/sat condition, where the threshold pores size between water-filled pores
170 at this matric potential is 15 μm . The matric potential corresponding to SAT/sat was obviously 0 kPa,
171 to give full saturation of all the pores. To calculate the intermediate HALFSAT/sat condition, we took
172 the mid-point gravimetric water content between 0 and -20 kPa from the water release characteristic,
173 and calculated the corresponding matric potential using Eq. [1], which was -8.6 kPa. We also
174 calculated the mid-point gravimetric water content between that at -20 kPa and θ_r , and found the
175 corresponding matric potential (Eq. [1]) to be -78.1 kPa. We used this to represent the UNSAT/halfsat
176 condition. As θ_r was non-zero (in fact it was 0.236 g g^{-1}), due to the fine-textured nature of the soil,
177 we accept that at -78.1 kPa the micropores were not truly half-saturated but would have been in a
178 wetter condition than this. However due to our method for equilibrating the soils prior to
179 experimentation, we required a suitable matric potential not lower than -1500 kPa that we could
180 control in the laboratory (see below). It could be argued that trying to attain a water content in the
181 hygroscopic range (that held at potentials much lower than -1500 kPa, often in the vapour phase),
182 where the true mid-point water content between that at -20 kPa and complete dryness in this soil lay,



183 was not especially relevant to denitrification processes expected in such a soil. There was one final
184 adjustment to make. The subsequent incubation experiment was to involve a 15 ml (3×5 ml) addition
185 of solution (see below). Through knowing masses and volumes of the solid-water-air phases of our
186 blocks, we therefore calculated revised matric potentials which would mean that the subsequent
187 addition of solution would achieve the target potentials given above. The target matric potentials of
188 0 (SAT/sat), -8.6 (HALFSAT/sat), -20.0 (UNSAT/sat) and -78.1 kPa (UNSAT/halfsat) were revised
189 to -4.1, -12.3, -27.3 and -136.9 kPa, respectively (see summary in Table 2). For the SAT/sat and
190 HALFSAT/sat conditions, two sets of three replicate blocks were placed on two fine-grade sand
191 tension tables connected to a water reservoir. For the UNSAT/sat condition a set of three replicate
192 blocks was placed on a tension plate connected to a water reservoir, and the final set of three replicate
193 blocks were placed in pressure plate chambers connected to high-pressure air. All blocks were
194 saturated on their respective apparatus for 24 h, and were then equilibrated for 7 days at the adjusted
195 target matric potentials which were achieved by either lowering the water level in the reservoir (sand
196 tables and tension plate) or by increasing the air pressure (pressure chambers). At the end of
197 equilibration period, the blocks were removed carefully from the apparatus, wrapped in air-tight film,
198 and maintained at 4 °C until the subsequent incubation.

199 **2.4 Incubation**

200 Each block containing three cores was placed in an individual incubation vessel of the automated
201 laboratory system described by Cardenas *et al.* (2003) in a randomised block design to avoid effect
202 of vessel. The lids for the vessels containing three holes were lined with the cores in the block to
203 ensure that the solution to be applied later would fall on top of each soil core. Stainless steel bulkheads
204 fitted (size for $\frac{1}{4}$ " tubing) on the lids had a three-layered Teflon coated silicone septum (4 mm thick
205 x 7 mm diameter) for supplying the amendment solution by using a gas tight hypodermic syringe.
206 The bulkheads were covered with a stainless steel nut and only open when amendment was applied.
207 The incubation experiment lasted 13 days. The incubation vessels with the soils were contained in a
208 temperature controlled cabinet and the temperature set at 20°C. The incubation vessels were flushed



209 from the bottom at a rate of 30 ml min^{-1} with a He/O₂ mixture (21% O₂, natural atmospheric
210 concentration) for 24 h, or until the system and the soils atmosphere were emitting low background
211 levels of both N₂ and N₂O (N₂ can get down to levels of 280 ppm much smaller than atmospheric
212 values). Subsequently, the He/O₂ supply was reduced to 10 ml min^{-1} and directed across the soil
213 surface and measurements of N₂O and N₂ carried out at approximately 2 hourly cycles to sample from
214 all the 12 vessels. Emissions of CO₂ were simultaneously measured.

215 **2.5 Application of amendment**

216 An amendment solution equivalent to 75 kg N ha^{-1} and 400 kg C ha^{-1} was applied as a 5 ml aliquot a
217 solution containing KNO₃ and glucose to each of the three cores in each vessel on day 0 of the
218 incubation. Glucose is added to optimise conditions for denitrification to occur (Morley and Baggs,
219 2010). The aliquot was placed in a stainless steel container (volume 1.2 l) which had three holes
220 drilled with bulkheads fitted, two to connect stainless steel tubing for flushing the vessel, and the third
221 one to place a septum on a bulkhead to withdraw solution. Flushing was carried out with He for half
222 an hour before the solution was required for application to the soil cores and continued during the
223 application process to avoid atmospheric N₂ contamination (a total of one and a half hours). The
224 amendment solution was manually withdrawn from the container with a glass syringe fitted with a
225 three-way valve onto the soil surface; care was taken to minimise contamination from atmospheric
226 N₂ entering the system. The syringe content was injected to the soil cores via the inlets on the lids
227 consecutively in each lid (three cores) and all vessels, completing a total of 36 applications that lasted
228 about 45 minutes. Incubation continued for twelve days, and the evolution of N₂O, N₂ and CO₂
229 measured continuously. At the end of each incubation experiment, the soils were removed from the
230 incubation vessels for further analysis. The three cores in each incubation vessel were pulled together
231 in one sample and subsamples taken and analysed for mineral N, total N and C and moisture status.
232 Table 3 shows the results of the soil analysis for all cores.



233 **2.6 Gas measurements**

234 Gas samples were directed to the relevant analysers via an automated injection valve fitted with 2
235 loops to direct the sample to two gas chromatographs. Emissions of N₂O and CO₂ were measured by
236 Gas Chromatography (GC), fitted with an Electron Capture Detector (ECD) and separation achieved
237 by a stainless steel packed column (2 m long, 4 mm bore) filled with 'Porapak Q' (80–100 mesh) and
238 using N₂ as the carrier gas. The detection limit for N₂O was equivalent to 2.3 g N ha⁻¹ d⁻¹. The N₂ was
239 measured by GC with a He Ionisation Detection (HID) and separation achieved by a PLOT column
240 (30 m long 0.53 mm i.d.), with He as the carrier gas. The detection limit was 9.6 g N ha⁻¹ d⁻¹. The
241 response of the two GCs was assessed by measuring a range of concentrations for N₂O, CO₂ and N₂.
242 Parent standards of the mixtures 10133 ppm N₂O + 1015.8 ppm N₂; 501 ppm N₂O + 253 ppm N₂ and
243 49.5 ppm N₂O + 100.6 ppm N₂ were diluted by means of Mass Flow controllers with He to give a
244 range of concentrations of: for N₂O of up to 750 ppm and for N₂ 1015 ppm. For CO₂ a parent standard
245 of 30,100 ppm was diluted down to 1136 ppm (all standards were in He as the balance gas). Daily
246 calibrations were carried out for N₂O and N₂ by using the low standard and doing repeated
247 measurements. The temperature inside the refrigeration cabinet containing the incubation vessels was
248 logged on an hourly basis and checked at the end of the incubation. The gas outflow rates were also
249 measured and recorded daily, and subsequently used to calculate the flux.

250 **2.7 Measurement of N₂O isotopic signatures**

251 Gas samples for isotopologue analysis were collected in 115 ml serum bottles sealed with grey butyl
252 crimp-cap septa (Part No 611012, Altmann, Holzkirchen, Germany). The bottles were connected by
253 a Teflon tube to the end of the chamber vents and were vented to the atmosphere through a needle, to
254 maintain flow through the experimental system. Dual isotope and isotopomer signatures of N₂O, i.e.
255 δ¹⁸O of N₂O (δ¹⁸O-N₂O), average δ¹⁵N (δ¹⁵N^{bulk}) and δ¹⁵N from the central N-position (δ¹⁵N^a) were
256 analysed after cryo-focussing by isotope ratio mass spectrometry as described previously (Well *et al.*,
257 2008). ¹⁵N site preference (SP) was obtained as SP = 2 * (δ¹⁵N^a – δ¹⁵N^{bulk}). Dual isotope and
258 isotopomer ratios of a sample (R_{sample}) were expressed as ‰ deviation from ¹⁵N/¹⁴N and ¹⁸O/¹⁶O ratios



259 of the reference standard materials (R_{std}), atmospheric N_2 and standard mean ocean water (SMOW),
260 respectively:

261
$$\delta X = (R_{sample}/R_{std} - 1) \times 1000 \quad [2]$$

262 where $X = {}^{15}N^{bulk}$, ${}^{15}N^a$, ${}^{15}N^b$, or ${}^{18}O$

263 **2.8 Data analysis and additional measurements undertaken**

264 The areas under the curves for the N_2O , CO_2 and N_2 data were calculated by using GenStat 11 (VSN
265 International Ltd, Hemel Hempstead, Herts, UK). The resulting areas for the different treatments were
266 analysed by applying analysis of variance (ANOVA). The isotopic (${}^{15}N^{bulk}$, ${}^{18}O$, and site preference
267 (SP) differences between the four treatment for the different sampling dates were analysed by two-
268 way ANOVA. We also used the Student's t test to check for changes in soil water content over the
269 course of the experiments.

270 Calculation of the relative contribution of the N_2O derived from bacterial denitrification
271 ($\%B_{DEN}$) was done according to Lewicka-Szczebak *et al.* (2015). The isotopic value of initially
272 produced N_2O , *i.e.* prior to its partial reduction (δ_0) was determined using a Rayleigh model (Mariotti
273 *et al.*, 1982), were δ_0 is calculated using the fractionation factor of N_2O reduction (η_{N2O-N2}) for SP and
274 the fraction of residual N_2O (f_{N2O}) which is equal to the $N_2O/(N_2+N_2O)$ product ratio obtained from
275 direct measurements of N_2 and N_2O flux. An endmember mixing model is then used to calculate the
276 percentage of bacterial N_2O in the total N_2O flux ($\%B_{DEN}$) from calculated δ_0 values and the SP and
277 $\delta^{18}O$ endmember values of bacterial denitrification and fungal denitrification/nitrification. The range
278 in endmember and η_{N2O-N2} values assumed (adopted from Lewicka-Szczebak, 2016a) to calculated
279 maximum and minimum estimates of $\%B_{DEN}$ is given in Table 4.

280 Because both, endmember values and η_{N2O-N2} values are not constant but subject to the given
281 ranges, we calculated here several scenarios using combinations of maximum, minimum and average
282 endmember and η_{N2O-N2} values (Table 4) to illustrate the possible range of $\%B_{DEN}$ for each sample.
283 For occasional cases where $\%B_{DEN} > 100\%$ the values were set to 100%.



284 At the same time as preparing the main soil blocks, a set of replicate samples was prepared in
285 exactly the same manner, but in smaller cores (i.d: 50 mm; h: 25 mm). On these samples we analysed
286 soil mineral N, total N and C and moisture at the start of the incubation. The same parameters were
287 measured after incubation by doing destructive sampling from the cores. Mineral N (NO_3^- , NO_2^- and
288 NH_4^+) was analysed after extraction with KCl by means of a segmented flow analyser using a
289 colorimetric technique (Searle, 1984). Total C and N in the air dried soil were analysed using a
290 thermal conductivity detector (TCD, Carlo Erba, model NA2000). Soil moisture was determined by
291 gravimetric analysis after drying at 105°C.

292 **3 Results**

293 **3.1 Soil composition**

294 The results after moisture adjustment at the start of the experiment resulted in a range of WFPS of
295 100 to 71% for the 4 treatments (Table 2). The results from the end of the incubation also showed
296 that there remained significant differences in soil moisture between the high moisture treatments
297 (SAT/sat and HALFSAT/sat) and the two lower moisture treatments (Table 3; one-way ANOVA,
298 $p<0.05$). Soil in the two wettest states lost statistically significant amounts of water (10% ($p=0.006$)
299 and 4.4% ($p<0.001$) for SAT/sat and HALFSAT/sat, respectively) over the course of the 13-day
300 incubation experiment. This was inevitable as there was no way to hold a high (near-saturation) matric
301 potential once the soil was inside the DENIS assembly, and water would have begun to drain by
302 gravitational forces out of the largest macropores ($>30\ \mu\text{m}$). An additional factor was the continuous
303 He/O_2 delivery over the soil surface which would have caused some drying. We accepted these as
304 unavoidable features of the experimental set-up, but we suggest that the main response of the gaseous
305 emissions occurred under the initial conditions, prior to the loss of water over subsequent days. Soil
306 in the two drier conditions had no significant change in their water content over the experimental
307 period ($p= 0.153$ and 0.051 for UNSAT/sat and UNSAT/halfsat, respectively). The results of the
308 initial soil composition were, for mineral N: $85.5\ \text{mg}\ \text{NO}_3^--\text{N}\ \text{kg}^{-1}$ dry soil, $136.2\ \text{mg}\ \text{NH}_4^+-\text{N}\ \text{kg}^{-1}$ dry
309 soil. The mineral N contents of the soils at the end of the incubation are reported in Table 3 showing



310 that NO_3^- was very small in treatments SAT/sat and HALFSAT/sat ($\sim 1 \text{ mg N kg}^{-1}$ dry soil) compared
311 to UNSAT/sat and UNSAT/halfsat ($50\text{--}100 \text{ N kg}^{-1}$ dry soil) at the end of the incubation. Therefore,
312 there was a significant difference in soil NO_3^- between the former, high moisture treatments and the
313 latter drier (UNSAT) treatments which were also significantly different between themselves ($p < 0.001$
314 for both). The NH_4^+ content was similar in treatments SAT/sat, HALFSAT/sat and UNSAT/sat (~ 100
315 mg N kg^{-1} dry soil), but slightly lower in treatment UNSAT/halfsat ($71.3 \text{ mg N kg}^{-1}$ dry soil), however
316 overall differences were not significant ($p > 0.05$).

317 **3.2 Gaseous emissions of N_2O , CO_2 and N_2**

318 The results showed that for treatments SAT/sat and HALFSAT/sat all three gases, N_2O , CO_2 and N_2
319 showed fluxes that were well replicated for all the vessels (see Fig. 1), in contrast for UNSAT/sat and
320 UNSAT/halfsat the emissions between the various replicated vessel in each treatment was not as
321 consistent, leading to a larger within treatment variability in the magnitude and shape of the GHG
322 fluxes measured. The cumulative fluxes also resulted in larger variability for the drier treatments
323 (Table 3).

324 *Nitrous oxide and nitrogen gas.* The general trend was that the N_2O concentrations in the
325 headspace increased shortly after the application of the amendment (Fig. 1). The duration of the N_2O
326 peak for each replicate soil samples was about three days, except for UNSAT/halfsat in which one of
327 the replicate soils exhibit a peak which lasted for about 5 days. The N_2O maximum in the SAT/sat
328 and HALFSAT/sat treatments was of similar magnitude (ca. $5.5 \text{ kg N ha}^{-1} \text{ d}^{-1}$) and those of
329 UNSAT/sat and UNSAT/halfsat also were comparable (at around $7 \text{ kg N ha}^{-1} \text{ d}^{-1}$). The N_2
330 concentrations always increased before the soil emitted N_2O reached the maximum. The lag between
331 both N_2O and N_2 peak for all samples was only few hours. Peaks of N_2 generally lasted just over four
332 days, except in UNSAT/halfsat where one replicate lasted about 6 days (Fig. 1). Unlike in the N_2O
333 data, there was larger within treatment variability in the replicates for all four treatments. The standard
334 deviations of each mean (Table 3) also indicate the large variability in treatments UNSAT/sat and
335 UNSAT/halfsat for both N_2O and N_2 .



336 The product ratios, i.e. $\text{N}_2\text{O}/(\text{N}_2\text{O}+\text{N}_2)$ showed a peak just after amendment addition by ca.
337 0.73 (at 0.49 d), 0.65 (at 0.48 d), 0.99 (at 0.35 d) and 0.88 (at 0.42 d) for SAT/sat, HALFSAT/sat,
338 UNSAT/sat and UNSAT/halfsat, respectively, and then decreases gradually until day 3 where it
339 becomes nearly zero for the 2 wettest treatments, and stays stable for the driest treatments between
340 0.1-0.2 (see Table 5 showing the daily means of these ratios).

341 The cumulative areas of the N_2O and N_2 peaks analysed by one-way ANOVA resulted in no
342 significant differences between treatments for both N_2O and N_2 (Table 3). Due to the large variation
343 in treatments UNSAT/sat and UNSAT/halfsat we carried out a pair wise analysis by using a weighted
344 t-test (Cochran, 1957). This analysis showed treatment differences between SAT/sat and
345 HALFSAT/sat, HALFSAT/sat and UNSAT/sat, SAT/sat and UNSAT/sat, but only at the 10%
346 significance level ($P < 0.1$ for both N_2O and N_2). It is possible that gases were trapped (particularly in
347 the higher saturation treatments) due to low diffusion and thus possibly masked differences in N_2 and
348 N_2O production since this fraction of gases was not detected (Harter et al. 2016).

349 The results showed that the total N emission ($\text{N}_2\text{O}+\text{N}_2$) (Table 3) had a consistent decreasing
350 trend, with decreasing soil moisture i.e. from 63.4 for SAT/sat (100% WFPS) to 34.1 kg N ha^{-1} (71%
351 WFPS) for UNSAT/halfsat. The maximum cumulative N_2O occurred at around 80% WFPS as Fig. 2
352 shows. The total $\text{N}_2\text{O}+\text{N}_2$ was largest at about 95% and for N_2 it was our upper treatment at 100%
353 WFPS.

354 *Carbon dioxide.* The background CO_2 values (before amendment application, i.e. day -1 to
355 day 0) were high at around $30 \text{ kg C ha}^{-1} \text{ d}^{-1}$ and variable (not shown). The CO_2 concentrations in the
356 headspace increased within a few hours after amendment application. The maximum CO_2 flux was
357 reached earlier in the drier treatments (about 1-2 days; $\sim 70 \text{ kg C ha}^{-1} \text{ d}^{-1}$) compared to the wettest (3
358 days; $\sim 40 \text{ kg C ha}^{-1} \text{ d}^{-1}$) and former peaks were also sharper (Fig. 1). The cumulative CO_2 fluxes were
359 significantly larger in the two drier unsaturated treatments (ca. $400-420 \text{ kg C ha}^{-1}$) when compared to
360 the wetter more saturated treatment (ca. $280-290 \text{ kg C ha}^{-1}$, $P < 0.05$) (Table 3).



361 **3.3 Isotopologues of N₂O**

362 The $\delta^{15}\text{N}^{\text{bulk}}$ of the soil emitted N₂O in our study differed significantly among the four treatments and
363 between the seven sampling dates (p<0.001 for both); there was also a significant treatment*sampling
364 date interaction (p<0.001). The maximum $\delta^{15}\text{N}^{\text{bulk}}$ generally occurred on day 3, except for SAT/sat
365 on day 4 (Table 6).

366 The maximum $\delta^{18}\text{O-N}_2\text{O}$ values were also found on day 3, except for SAT/sat which peaked
367 at day 2 (Table 6). Overall, the $\delta^{18}\text{O-N}_2\text{O}$ values varied significantly between treatment and sampling
368 dates (p<0.001 for both), but there was no significant treatment*time interaction (p>0.05).

369 The site preference (SP) showed for the SAT/sat treatment an initial maximum value on day 2 (6.3‰)
370 which decreased thereafter in period from day 3 to 5 to a mean SP values of the emitted N₂O of 2.0‰
371 on day 5, subsequently rising to 8.4‰ on day 12 of the experiment (Table 6). The HALFSAT/sat
372 treatment had the highest initial SP values on day 2 and 3 (both 6.4‰), decreasing again to a value
373 of 2.0‰, but now already on day 4 followed by subsequent higher SP values of up to 9.2‰ on day 7
374 (Table 6). The two driest treatments (UNSAT/sat and UNSAT/halfsat) both showed an initial
375 maximum on day 3 (11.9‰ and 5.9‰, respectively), and in UNSAT/sat the SP value then decreased
376 to day 7 (3.9‰), but in UNSAT/halfsat treatment after a marginal decrease on day 4 (5.4‰) it then
377 increased throughout the experiment reaching 11.8‰ on day 12 (Table 6). The lowest SP values were
378 generally on day 1 in all treatments. Overall, for all parameters, there was more similarity between
379 the more saturated treatments SAT/sat and HALFSAT/sat, and between the two more dry and aerobic
380 treatments UNSAT/sat and UNSAT/halfsat.

381 The plot of the N₂O / (N₂O + N₂) ratio vs SP for all treatments in the first two days (when
382 N₂O was increasing and the N₂O / (N₂O + N₂) ratio was decreasing) shows a significant negative
383 response of the SP when the ratio increased (Fig. 3). The regression suggests that when the emitted
384 gaseous N is dominated by N₂O (ratio close to 1) the SP values will be slightly negative with values
385 around -2 (Fig. 3). This is in juxtaposition with the situation when the N emissions are dominated by
386 N₂ or N₂O is low, where the SP values of soil emitted N₂O were much higher (Fig. 3), pointing to an



387 overall product ratio related to an ‘isotopic shift’ of 10 to 12.5‰. We fitted 3 functions through this
388 data including a second degree polynomial, a linear and logarithmic function. The fitted logarithmic
389 function, shown in Fig. 3, is in almost perfect agreement with Lewicka-Szczebak *et al.* (2014).
390 Lewicka-Szczebak *et al.* (2014) data fits on the top left of Fig. 3 (their values are for SP and ratio
391 $N_2O / (N_2O + N_2)$: 18.5, 0.18; 10.1, 0.19; 11, 0.28 and 13.4, 0.24, respectively).

392 It has been reported that the combination of the isotopic signatures of N_2O potentially
393 identifies the contribution of processes other than bacterial denitrification (Köster *et al.*, 2015; Wu
394 Di *et al.*, 2016; Deppe *et al.*, 2017) so we have carried out similar analysis with our data. The
395 maximum $\delta^{18}O$ and SP values, were generally observed at or near the peak of N_2 emissions on days
396 2-3, independent of the moisture treatment (Table 6 and Fig. 3). $\delta^{15}N^{bulk}$ values of all treatments were
397 mostly negative when N_2O fluxes started to increase (day 1, Fig. 1, Table 6), except for
398 UNSAT/halfsat in which the lowest value was before amendment application, reaching their highest
399 values between days 3 and 4 for when N_2O fluxes were back to the low initial values, and then
400 decreased during the remaining period. $\delta^{18}O$ values increased about 10 - 20‰ after day 1 reaching
401 maximum values on days 2 or 3 in all treatments, while SP increased in parallel, at least by 3‰
402 (SAT/sat) and up to 12‰(UNSAT/sat). While $\delta^{18}O$ exhibited a steady decreasing trend after day 3,
403 SP behaved opposite to $\delta^{15}N^{bulk}$ with decreasing values while $\delta^{15}N^{bulk}$ was rising again after days 4 or
404 5.

405 We further explored the data by looking at the relationships between the $\delta^{18}O$ and $\delta^{15}N^{bulk}$ for
406 all the treatments. Figure 4 shows the $\delta^{18}O$ vs $\delta^{15}N^{bulk}$ for all treatments separating the data in three
407 periods: ‘-1’, with $\delta^{18}O$ vs $\delta^{15}N^{bulk}$ values 1 day prior to the moisture adjustment (and N and C
408 application); ‘1-2’, with values in the first 2 days after the addition of water, N and C were added and
409 N_2O emissions were generally increasing in all treatments; and, ‘3-12’, the period in days after
410 moisture adjustment and N and C addition when N_2O emissions generally decreased back to baseline
411 soil emissions. There was a strong relationship between $\delta^{18}O$ vs $\delta^{15}N^{bulk}$ for the high moisture
412 treatments ($R^2 = 0.973$ and 0.923 for SAT/sat and HALFSAT/sat, respectively) at the beginning of



413 the incubation ('1-2') when the N_2O emissions are still increasing, in contrast to those of the lower
414 soil moisture treatments that were lower ($R^2 = 0.294$ and 0.622, for UNSAT/sat and UNSAT/halfsat,
415 respectively). The relationships between $\delta^{18}\text{O}$ vs $\delta^{15}\text{N}^{\text{bulk}}$ of emitted N_2O for the '3-12' period have
416 R^2 values between 0.549 and 0.896 (Fig. 4). Interestingly, with decreasing soil moisture content (Fig.
417 4a to 4d) the regression lines of '1-2' and '3-12' day period got closer together in the plotted graphs.
418 Overall, the $\delta^{15}\text{N}^{\text{bulk}}$ isotopic distances between the two lines was larger for a given $\delta^{18}\text{O}-\text{N}_2\text{O}$ value
419 for SAT/sat and HALFSAT/sat (ca. 20‰) when compared to the UNSAT/sat and UNSAT/halfsat
420 treatments (ca. 13‰) (Fig. 4). So it seems the $\delta^{15}\text{N}^{\text{bulk}} / \delta^{18}\text{O}-\text{N}_2\text{O}$ signatures are more similar for the
421 drier soil than the two wettest treatments. In addition, Fig 4 exactly reflects the 2-pool dynamics with
422 increasing $\delta^{15}\text{N}$ and $\delta^{18}\text{O}$ while the product ratio goes down (days 2,3), then only $\delta^{15}\text{N}$ continue
423 increasing due to fractionation of the NO_3^- during exhaustion of pool 1 in the wet soil (days 3,4,5),
424 finally as pool 1 is depleted and more and more comes from pool 2, the product ratio increases
425 somewhat, and $\delta^{15}\text{N}$ decreases somewhat since pool 2 is less fractionated and also $\delta^{18}\text{O}$ decreases due
426 to slightly increasing product ratio. Note that the turning points of $\delta^{18}\text{O}$ and product ratio (Table 3
427 and 4) for the wetter soils almost coincide.

428 Similarly to Fig. 4, we plotted the $\delta^{18}\text{O}$ vs the SP (Fig. 5) for the different phases of the
429 experiment. Generally, the slopes (Table 7) for days 1-2 for the three wettest treatments were similar
430 (~0.2-0.3) following the range of known reduction slopes and also had high regression coefficients
431 ($R^2 = 0.65$, 0.90 and 0.87 for SAT/sat, HALFSAT/Sat and UNSAT/sat, respectively). The slopes on
432 days 3-5 were variable but slightly similar on days 7-12 (between 41 and 0.68) for the same three
433 treatments. Figure 5 also shows the "map" for the values of SP and $\delta^{18}\text{O}$ from all treatments.
434 Reduction lines (vectors) represent minimum and maximum routes of isotopologue values with
435 increasing N_2O reduction to N_2 based on the reported range in the ratio between the isotope
436 fractionation factors of N_2O reduction for SP and $\delta^{18}\text{O}$ (Lewicka-Szczebak *et al.*, (2016a) Most
437 samples are located within the vectors (from Lewicka-Szczebak *et al.* 2016a) area of N_2O production
438 by bacterial denitrification with partial N_2O reduction to N_2 (within uppermost and lowermost N_2O



439 reduction vectors representing the extreme values for the bacterial endmember and reduction slopes).

440 Only a few values of the UNSAT/sat and UNSAT/halfsat treatments are located above that area and
441 more close or within the area of mixing between bacterial denitrification and fungal
442 denitrification/nitrification.

443 The estimated ranges of the proportion of emitted N_2O resulting from bacterial denitrification
444 ($\% \text{B}_{\text{DEN}}$) were on day 1 and 2 after the amendment comparable in all four moisture treatments (Table
445 6). However, during day 3 to 12 the $\% \text{B}_{\text{DEN}}$ ranged from 78-100% in SAT/sat and 79-100%
446 HALFSAT/Sat, which was generally higher than that estimated at 54-86% for UNSAT/halfsat
447 treatment. The $\% \text{B}_{\text{DEN}}$ of the UNSAT/halfsat in that period was intermediate between SAT/sat and
448 UNSAT/sat with range of range 60-100% (Table 6). The final values were similar to those on day -1
449 except for the UNSAT/sat treatment.

450 4 Discussion

451 4.1 N_2O and N_2 fluxes

452 The observed decrease in total N emissions with decreasing soil moisture reflects the effect of soil
453 moisture as reported in previous studies (Well *et al.*, 2006). The differences when comparing the
454 cumulative fluxes however, were only marginally ($p < 0.1$) significant (Table 3) mostly due to large
455 variability within replicates in the drier treatments (see Fig. 1b). Davidson *et al.* (1991) provided a
456 WFPS threshold for determination of source process, with a value of 60% WFPS as the borderline
457 between nitrification and denitrification as source processes for N_2O production. The WFPS in all
458 treatments in our study was larger than 70%, above this 60% threshold, and referred to as the
459 “optimum water content” for N_2O by Scheer *et al.* (2009), so we can be confident that denitrification
460 was likely to have been the main source process in our experiment. In addition, Bateman *et al.* (2004)
461 observed the largest N_2O fluxes at 70% WFPS on a silty loam soil, lower than the 80% value for the
462 largest fluxes from the clay soil in our study (Fig. 2) suggesting that this optimum value could change
463 with soil type. Further, the maximum total measured N lost ($\text{N}_2\text{O} + \text{N}_2$) in our study occurred at about
464 95% WFPS (Fig. 2), but not many studies report N_2 fluxes for comparison and we are still missing



465 measurements of nitric oxide (NO) (Davidson *et al.*, 2000) and ammonia (NH₃) to account for the
466 total N losses. It is however possible that the N₂O+N₂ fluxes in the SAT/sat treatment were
467 underestimated due to low diffusivity in the water filled pores (Well *et al.*, 2001).

468 The smaller standard errors in both N₂O and N₂ data for the larger soil moisture levels (Table
469 3 and Fig. 1) could suggest that at high moisture contents nutrient distribution (N and C) on the top
470 of the core is more homogeneous making replicate cores to behave similarly. At the lower soil
471 moisture for both N₂O and N₂, it is possible that some cracks appear on the soil surface causing
472 downwards nutrient movement, resulting in heterogeneity in nutrient distribution on the surface and
473 increasing variability between replicates, reflected in the larger standard errors of the fluxes. Laudone
474 *et al.* (2011) studied, using a biophysical model, the positioning of the hot-spot zones away from the
475 critical percolation path (described as 'where air first breaks through the structure as water is removed
476 at increasing tensions') and found it slowed the increase and decline in emission of CO₂, N₂O and N₂.
477 They found that hot-spot zones further away from the critical percolation path would reach the
478 anaerobic conditions required for denitrification in shorter time, the products of the denitrification
479 reactions take longer to migrate from the hot-spot zones to the critical percolation path and to reach
480 the surface of the system. The model and its parameters can be used for modelling the effect of soil
481 compaction and saturation on the emission of N₂O. They suggest that having determined biophysical
482 parameters influencing N₂O production, it remains to determine whether soil structure, or simply
483 saturation, is the determining factor when the biological parameters are constrained. Furthermore,
484 Clough *et al.* (2013) indicate that microbial scale models need to be included on larger models linking
485 microbial processes and nutrient cycling in order to consider spatial and temporal variation. Kulkarni
486 *et al.* (2008) refers to "hot spots" and "hot moments" of denitrification as scale dependant and
487 highlight the limitations for extrapolating fluxes to larger scales due to these inherent variabilities.
488 Well *et al.* (2003) found that under saturated conditions there was good agreement between laboratory
489 and field measurements of denitrification, and attributed deviations, under unsaturated conditions, to
490 spatial variability of anaerobic microsites and redox potential. Dealing with spatial variability when



491 measuring N₂O fluxes in the field remains a challenge, but the uncertainty could be potentially
492 reduced if water distribution is known. Our laboratory study suggests that soil N₂O and N₂ emission
493 for higher moisture levels would be less variable than for drier soils and suggests that for the former
494 a smaller number of spatially defined samples will be needed to get an accurate field estimate.

495 Our results, for the two highest water contents (SAT/sat and HALFSAT/sat), showed that N₂O
496 only contributed 20% of the total N emissions, as compared to 40-50% at the lowest water contents
497 (UNSAT/sat and UNSAT/halfsat, Table 3). This was due to reduction to N₂ at the high moisture level,
498 confirmed by the larger N₂ fluxes, favoured by low gas diffusion which increased the N₂O residence
499 time and the chance of further transformation (Kleftho *et al.*, 2014a). We should also consider the
500 potential underestimation of the fluxes in the highest saturation treatment due to restricted diffusion
501 in the water filled pores (Well *et al.*, 2001). A total of 99% of the soil NO₃⁻ was consumed in the two
502 high water treatments, whereas in the drier UNSAT/sat and UNSAT/halfsat treatments there still was
503 35% and 70% of the initial amount of NO₃⁻ left in the soil, at the end of the incubation, respectively
504 (Table 3). The total amount of gas lost compared to the NO₃⁻ consumed was almost 3 times for the
505 wetter treatments, and less than twice for the 2 drier ones. This agrees with denitrification as the
506 dominant process source for N₂O with larger consumption of NO₃⁻ at the higher moisture and larger
507 N₂ to N₂O ratios (5.7, 4.7 for SAT/sat and HALFSAT/sat, respectively), whereas at the lower
508 moisture, ratios were lower (1.5 and 1.0 for UNSAT/sat and UNSAT/halfsat, respectively) (Davidson,
509 1991). This also indicates that with WFPS above the 60% threshold for N₂O production from
510 denitrification, there was an increasing proportion of anaerobic microsites with increase in saturation
511 controlling NO₃⁻ consumption and N₂/N₂O ratios in an almost linear manner. With WFPS values
512 between 71-100 % and N₂/N₂O between 1.0 and 5.7, a regression can be estimated: Y=0.1723 X –
513 11.82 (R²=0.8585), where Y is N₂/N₂O and X is %WPS. In summary, we propose that
514 heterogeneous distribution of anaerobic microsites could have been the limiting factor for complete
515 depletion of NO₃⁻ and conversion to N₂O in the two drier treatments. In addition, in the
516 UNSAT/halfsat treatment there was a decrease in soil NH₄⁺ at the end of the incubation (almost 50%;



517 Table 3) suggesting nitrification could have been occurring at this water content which also agrees
518 with the increase in NO_3^- , even though WFPS was relatively high (>71%) (Table 3). It is important
519 to note that as we did not assess gross nitrification, the observed net nitrification based on lowering
520 in NH_4^+ could underestimate gross nitrification since there might have been substantial N
521 mineralisation during the incubation. However, under conditions favouring denitrification at high soil
522 moisture the typical N_2O produced from nitrification is much lower compared to that from
523 denitrification (Lewicka-Szczebak *et al.*, 2016a) with the maximum reported values for the N_2O yield
524 of nitrification of 1-3 % (e.g. Deppe *et al.*, 2017). If this is the case, nitrification fluxes could not have
525 exceeded 1 kg N with NH_4^+ loss of < 30 kg * 3% ~1 kg N. This would have represented for the driest
526 treatment, if conditions were suitable only for one day, that nitrification-derived N_2O would have
527 been 6% of the total N_2O produced. Loss of NH_3 was not probable at such low pH (5.6). The
528 corresponding rate of NO_3^- production using the initial and final soil contents and assuming other
529 processes were less important in magnitude, would have been < 1 mg NO_3^- -N kg dry soil⁻¹ d⁻¹ which
530 is a reasonable rate (Hatch *et al.*, 2002). The other three treatments lost similar amounts of soil NH_4^+
531 during the incubation (23-26%) which could have been due to some degree of nitrification at the start
532 of the incubation before O_2 was depleted in the soil microsites or due to NH_4^+ immobilisation (Table
533 3) (Geisseler *et al.*, 2010).

534 The CO_2 released in all treatments supports the statement above in relation with the more
535 aerobic status of UNSAT/sat and UNSAT/halfsat, because the cumulative CO_2 flux is roughly 1.5
536 times higher in the two drier treatments when compared to the wetter ones; but it could have also
537 been the result of higher diffusion in the drier treatments.

538 A mass N balance, taking into account the initial and final soil NO_3^- , NH_4^+ , added NO_3^- and
539 the emitted N (as N_2O and N_2) results in unaccounted N-loss of 177.2, 177.6, 130.6 and 110.8 mg N
540 kg⁻¹ for SAT/sat, HALFSAT/sat, UNSAT/sat and UNSAT/halfsat, respectively, that could have been
541 emitted as other N gases (such as NO), and some, immobilised in the microbial biomass. In addition,



542 in the SAT/sat treatment there was probably an underestimation of the produced N_2 and N_2O due to
543 restricted diffusion at the high WFPS (e.g. Well *et al.*, 2001).

544 **4.2 Isotopologue trends.**

545 Trends of isotopologue values of emitted N_2O coincided with those of N_2 and N_2O fluxes. The results
546 from the isotopomer data (Table 6 and Fig. 3) also showed that generally there were more isotopic
547 similarities between the two wettest treatments when compared to the two contrasting drier soil
548 moisture treatments.

549 Isotopologue values of emitted N_2O reflect multiple processes where all signatures are
550 affected by the admixture of several microbial processes, the extent of N_2O reduction to N_2 as well
551 as the variability of the associated isotope effects (Lewicka-Szczebak *et al.*, 2015). Moreover, for
552 $\delta^{18}\text{O}$ and $\delta^{15}\text{N}^{\text{bulk}}$ the precursor signatures are variable (Decock and Six, 2013), for $\delta^{18}\text{O}$ the O
553 exchange with water can be also variable (Lewicka-Szczebak *et al.*, 2016b). Since the number of
554 influencing factors clearly exceeds the number of isotopologue values, unequivocal results can only
555 be obtained if certain processes can be excluded or be determined independently, (Lewicka-Szczebak
556 *et al.*, 2015; Lewicka-Szczebak, 2016a). The two latter conditions were fulfilled in this study, i.e.
557 N_2O fluxes were high and several order of magnitude above possible nitrification fluxes, since the
558 N_2O – to- NO_3^- ratio yield of nitrification products rarely exceeds 1% (Well *et al.*, 2008; Zhu *et al.*,
559 2012). Moreover, N_2 fluxes and thus N_2O reduction rates were exactly quantified.

560 The estimated values of % B_{DEN} showed that in the period immediately after amendment
561 application all moisture treatments were similar, reflecting that the microbial response to N and C
562 added was the same and denitrification dominated. This was the same for the rest of the period for
563 the wetter treatments. In the drier treatments, proportions decreased afterwards and were similar to
564 values before amendment application, possibly due to recovery of more aerobic conditions that could
565 have encouraged other processes to contribute. As N_2 was still produced in the driest treatment, (but
566 in smaller amounts), this indicated ongoing denitrifying conditions and thus large contributions from
567 nitrification were not probable, but some occurred as suggested by NH_4^+ consumption.



568 The trends observed reflect the dynamics resulting from the simultaneous application of
569 NO_3^- and labile C (glucose) on the soil surface as described in previous studies (Meijide *et al.*,
570 2010; Bergstermann *et al.*, 2011) where the same soil was used, resulting in two locally distinct
571 NO_3^- pools with differing denitrification dynamics. In the soil volume reached by the NO_3^- /glucose
572 amendment, denitrification was initially intense with high N_2 and N_2O fluxes and rapid isotopic
573 enrichment of the NO_3^- -N. When the NO_3^- and/or glucose of this first pool were exhausted, N_2 and
574 N_2O fluxes were much lower and dominated by the initial NO_3^- pool that was not reached by the
575 glucose/ NO_3^- amendment and that is less fractionated due to its lower exhaustion by denitrification,
576 causing decreasing trends in $\delta^{15}\text{N}^{\text{bulk}}$ of emitted N_2O .

577 This is also reflected in Fig 4 showing that N_2O fluxes from both pools exhibited correlations
578 between $\delta^{15}\text{N}^{\text{bulk}}$ and $\delta^{18}\text{O}$ due to varying N_2O reduction, but $\delta^{15}\text{N}^{\text{bulk}}$ values in days 1 and 2 - i.e. the
579 phase when Pool 1 dominated - were distinct from the previous and later phase.

580 The fit of $^{15}\text{N}^{\text{bulk}}$ / ^{18}O data to two distinct and distant regression lines can be attributed to
581 two facts: Firstly, in the wet treatment (Fig 4a, b) Pool 1 was probably completely exhausted and
582 there was little NO_3^- formation from nitrification (indicated by final NO_3^- values close to 0, Table 3)
583 whereas the drier treatment exhibited substantial NO_3^- formation and high residual NO_3^- . Hence,
584 there was probably still some N_2O from Pool 1 after day 2 in the dry treatment but not in the wetter
585 ones. Secondly, the product ratios after day 2 of the drier treatments were higher (0.13 to 0.44)
586 compared to the wetter treatments (0.001 to 0.09). Thus the isotope effect of N_2O reduction was
587 smaller in the drier treatments, leading to a smaller upshift of $\delta^{15}\text{N}^{\text{bulk}}$ and thus more negative values
588 after day 2, i.e. with values closer to days 1 +2.

589 This finding further confirms that $\delta^{15}\text{N}/\delta^{18}\text{O}$ patterns are useful to identify the presence of
590 several N pools, e.g. typically occurring after application of liquid organic fertilizers which has
591 been previously demonstrated using isotopologue patterns (Koster *et al.*, 2015).

592 Interestingly, the highest $\delta^{15}\text{N}^{\text{bulk}}$ and $\delta^{18}\text{O}$ values of the emitted N_2O were found in the soils
593 of the HALFSAT/sat treatment, although it may have been expected that the highest isotope values



594 from the N₂O would be found in the wettest soil (SAT/sat) because N₂O reduction to N₂ is favoured
595 under water-saturated conditions due to extended residence time of produced N₂O (Well et al., 2012).
596 However, N₂O/(N₂+N₂O) ratios of the SAT/sat and SAT/halfsat treatments were not different (Table
597 5). Bol *et al.* (2004) also found that some estuarine soils under flooded conditions (akin to our
598 SAT/sat) showed some strong simultaneous depletions (rather than enrichments) of the emitted N₂O
599 δ¹⁵N^{bulk} and δ¹⁸O values. These authors suggested that this observation may have resulted from a flux
600 contribution of an ‘isotopically’ unidentified N₂O production pathway. Another explanation could be
601 complete consumption of some of the produced N₂O in isolated micro-niches in the SAT/sat treatment
602 due to inhibited diffusivity in the fully saturated pores space. N₂ formation in these isolated domains
603 would not affect the isotopologue values of emitted N₂O and this would thus result in lower apparent
604 isotope effects of N₂O reduction in water saturated environments as suggested by Well *et al.* (2012).

605 The SP values obtained were generally below 12‰ in agreement with reported ranges
606 attributed to bacterial denitrification: -2.5 to 1.8‰ (Sutka *et al.*, 2006); 3.1 to 8.9‰ (Well and
607 Flessa, 2009); -12.5 to 17.6‰ (Ostrom, 2011). The SP, believed to be a better predictor of the N₂O
608 source as it is independent of the substrate isotopic signature (Ostrom, 2011), has been suggested as
609 it can be used to estimate N₂O reduction to N₂ in cases when bacterial denitrification can be
610 assumed to dominate N₂O fluxes (Koster *et al.*, 2013; Lewicka-Szczebak *et al.*, 2015). There was a
611 strong correlation between the SP and N₂O / (N₂O+N₂) ratios on the first 2 days of the incubation
612 for all treatments up until the N₂O reached its maximum (Fig. 3) which reflects the accumulation of
613 δ¹⁵N at the alpha position during ongoing N₂O reduction to N₂. Later on in the experiment beyond
614 day 3, this was not observed probably because in that period the product ratio remained almost
615 unchanged and very low (Table 6). Similar observations have been reported by Meijide *et al.* (2010)
616 and Bergstermann *et al.* (2011), as they also found a decrease in SP during the peak flux period in
617 total N₂+N₂O emissions, but only when the soil had been kept wet prior to the start of the
618 experiment (Bergstermann *et al.*, 2011). These results confirm from 2 independent studies
619 (Lewicka-Szczebak *et al.*, 2014) that there is a relationship between the product ratios and isotopic



620 signatures of the N₂O emitted. The δ¹⁸O vs SP regressions showed more similarity between the
621 three wettest treatments as well as high regression coefficients, suggesting this SP/δ¹⁸O ratio could
622 also be used to help identify patterns for emissions and their sources.

623 **4.3 Link to modelling approaches.**

624 Since isotopologue data could be compared to N₂ and N₂O fluxes, the variability of isotope effects
625 of N₂O production and reduction to N₂ by denitrification could be determined from this data set
626 (Lewicka-Szczebak *et al.*, 2015). This included modelling the two pool dynamics discussed above.
627 It was shown that net isotope effects of N₂O reduction (η_{N₂O-N₂}) determined for both NO₃⁻ pools
628 differed. Pool 1 representing amended soil and showing high fluxes but moderate product ratio,
629 exhibited η_{N₂O-N₂} values and the characteristic η¹⁸O/η¹⁵N ratios similar to those previously reported,
630 whereas for Pool 2 characterized by lower fluxes and very low product ratio, the net isotope effects
631 were much smaller and the η¹⁸O/η¹⁵N ratios, previously accepted as typical for N₂O reduction
632 processes (i.e., higher than 2), were not valid.

633 The question arises, if the poor coincidence of Pool 2 isotopologue fluxes with previous
634 N₂O reduction studies reflects the variability of isotope effects of N₂O reduction or if the
635 contribution of other processes like fungal denitrification could explain this.

636 Liu *et al.* (2016) noted that on the catchment scale potential N₂O emission rates were
637 related to hydroxylamine and NO₃⁻, but not NH₄⁺ content in soil. Zou *et al.* (2014) found high SP
638 (15.0 to 20.1‰) values at WFPS of 73 to 89% suggesting that fungal denitrification and bacterial
639 nitrification contributed to N₂O production to a degree equivalent to that of bacterial denitrification.

640 To verify the contribution of fungal denitrification and/or hydroxylamine oxidation we can
641 first look at the η_{SP_{N₂O-NO₃}} values calculated in the previous modelling study applied on the same
642 dataset, (Table 1, the final modelling Step, Lewicka-Szczebak *et al.*, 2015). For Pool 1 there are no
643 significant differences between the values of various treatments, SP₀ ranges from (-1.8±4.9) to
644 (+0.1±2.5). Pool 1 emission was mostly active in days 1-2, hence these values confirm the bacterial
645 dominance in the emission at the beginning of incubation, which originates mainly from the



646 amendment addition and represent similar pathway for all treatments. However, for the Pool 2
647 emission we could observe a significant difference when compared the two wet treatments (SAT/sat
648 and HALFSAT/sat: (-5.6±7.0)) with the UNSAT/sat treatment (+3.8±5.8). This represents the
649 emission from unamended soil which was dominating after the third day of the incubation and
650 indicates higher nitrification contribution for the drier treatment.

651 **4.4 Contribution of bacterial denitrification.**

652 An endmember mixing approach has been previously used to estimate the fraction of bacterial N₂O
653 (%B_{DEN}), but without independent estimates of N₂O reduction (Zou *et al.*, 2014), but due to the
654 unknown isotopic shift by N₂O reduction, the ranges of minimum and maximum estimates were large,
655 showing that limited information is obtained without N₂ flux measurement.

656 In an incubation study with two arable soils, Koster *et al.* (2013) used N₂O/(N₂+N₂O) ratios
657 and isotopologue values of gaseous fluxes to calculate SP of N₂O production (referred to as SP₀),
658 which is equivalent to SP₀ using the Rayleigh model and published values of η_{N2O-N2} . The
659 endmember mixing approach based on SP₀ was then used to estimate fungal denitrification and/or
660 hydroxylamine oxidation giving indications for a substantial contribution in a clay soil, but not in a
661 loamy soil. Here we presented for the first time an extensive data set with large range in product
662 ratios and moisture to calculate the contribution of bacterial denitrification (%B_{DEN}) of emitted N₂O
663 from SP₀. The uncertainty of this approach arises from three factors, (i) from the range of SP₀
664 endmember values for bacterial denitrification of -11 to 0 per mil and 30 to 37 for hydroxylamine
665 oxidation/fungal denitrification, (ii) from the range of net isotope effect values of N₂O reduction
666 (η_{N2O-N2}) for SP which vary from -2 to -8 per mil (Lewicka-Szczebak *et al.*, 2015), and iii) system
667 condition (open vs. closed) taken to estimate the net isotope effect (Wu *et al.*, 2016).

668 The observation that %B_{DEN} of emitted N₂O was generally high (63-100%) in the wettest
669 treatment (SAT/sat) was not unexpected. However interestingly %B_{DEN} in the HALFSAT/sat
670 treatment was very similar (71-98%), pointing to the role of the wetter areas of the soil
671 microaggregates contributing to high %B_{DEN} values. The slightly lower values, i.e. down 60% in



672 UNSAT/sat %B_{DEN} range of 60-100%, suggest that the majority of N₂O derived from bacterial
673 denitrification still results from the wetter microaggregates of the soils, despite the fact that the
674 macropores are now more aerobic. Only, when the micropores become partially wet, as in the
675 UNSAT/halfsat treatment, do the more aerobic soil conditions allow a higher contribution of
676 nitrification/fungal denitrification ranging from 0 - 46% (1 - % B_{DEN}, Table 6) on days 3-12 (Zhu *et*
677 *al.*, 2013). Differences in the contribution of nitrification/fungal denitrification between the flux
678 phases when different NO₃⁻ pools were presumably dominating are only indicated in the driest
679 treatment, since 1-%B_{DEN} was higher after day 2 (14 to 46%) compared to days 1+2 (0 to 33 %).
680 This larger share of nitrification/fungal denitrification can be attributed to the increasing
681 contribution from Pool 2 to the total flux as indicated by the modeling of higher SP₀ for Pool 2 (see
682 previous section and Lewicka-Szczebak *et al.* (2015). In addition, indication for elevated
683 contribution of processes other than bacterial denitrification were only evident in the drier
684 treatments during phases before and after N₂, N₂O fluxes were strongly enhanced by glucose
685 amendment. The data supply no clue whether the other processes were suppressed during the anoxia
686 induced by glucose decomposition or just masked by the vast glucose-induced bacterial N₂O fluxes.
687

688 **5 Conclusions**

689 The results from this study showed that at high soil moisture levels, there was less variability in N
690 fluxes between replicates, potentially decreasing the importance of soil hot spots in emissions at
691 these moisture levels. At high moisture there also was complete depletion of nitrate confirming
692 denitrification as the main pathway for N₂O emissions, and due to less diffusion of the produced
693 N₂O, the potential for further reduction to N₂ increased. Under less saturation, but still relatively
694 high soil moisture, nitrification occurred. Isotopic similarities were observed between similar
695 saturation levels and patterns of δ¹⁵N/δ¹⁸O and SP/δ¹⁸O are suggested as indicators of source
696 processes.



697 **Acknowledgments**

698 The authors would like to thank the technical help from Mark Butler during the laboratory
699 incubation and Andrew Bristow and Patricia Butler for carrying out soil analysis. Also thanks to
700 Dan Dhanoa for advice on statistical analysis, and to Anette Giesemann and Martina Heuer for help
701 in N_2O isotopic analyses. This study was funded by the UK Biotechnology and Biological Sciences
702 Research Council (BBSRC) with competitive grants BB/E001580/1 and BB/E001793/1.
703 Rothamsted Research is sponsored by the BBSRC.

704

705



706 **Figures**

707 **Figure 1.** Mean of the three replicates for N_2O , N_2 and CO_2 emissions from a. SAT/sat treatment; b.
708 HALFSAT/sat; c. UNSAT/sat; d. UNSAT/halfsat. Grey lines correspond to the standard error of the
709 means.

710 **Figure 2** Total N emissions ($\text{N}_2\text{O} + \text{N}_2$)-N, N_2O and N_2 vs WFPS. Fitted functions through each
711 dataset are also shown.

712 **Figure 3** Ratio $\text{N}_2\text{O} / (\text{N}_2\text{O} + \text{N}_2)$ vs. Site Preference (SP) for all for treatments in the first two days.
713 A logarithmic function was fitted through the data, the corresponding equation and correlation
714 coefficient are given.

715 **Figure 4** $\delta^{18}\text{O}$ vs $\delta^{15}\text{N}_{\text{bulk}}$ in all treatments for three periods (day -1 in diamond symbol, days 1-2 in
716 square symbol and days 3-12 in triangle symbol, respectively) in the experiment: a. SAT/sat
717 treatment; b. HALFSAT/sat; c. UNSAT/sat; d. UNSAT/halfsat. Equations of fitted functions and
718 correlation coefficients are shown.

719 **Figure 5** Site Preference vs $\delta^{18}\text{O}$ in all treatments for three periods (day -1, days 1-2 and days 3-12)
720 in the experiment: a. SAT/sat treatment; b. HALFSAT/sat; c. UNSAT/sat; d. UNSAT/halfsat.
721 Equations of fitted functions and correlation coefficients are in Table 7 for 1-2, 3-5 and 7-12 (5-12
722 for c.). Endmember areas for nitrification, N; bacterial denitrification, D; fungal denitrification, FD
723 and nitrifier denitrification, ND and corresponding vectors or reduction lines (grey solid lines) are
724 from Lewicka-Szczebak et al., (2016a), and represent minimum and maximum routes of
725 isotopologue values with increasing N_2O reduction to N_2 based on the reported range in the ratio
726 between the isotope fractionation factors of N_2O reduction for SP and $\delta^{18}\text{O}$ (Lewicka-Szczebak et
727 al., 2016a).

728 **Tables**

729 **Table 1** Soil properties of the soil used in the experiment

730 **Table 2** The four saturation conditions used for the soil in the experiment



731 **Table 3** Contents of soil moisture, NO_3^- , NH_4^+ and C:N ratio and cumulative fluxes of N_2O and N_2
732 and CO_2 from all treatments at the end of the incubation.

733 **Table 4** Scenarios with different combinations of $\delta^{18}\text{O}$ and SP endmember values and $\eta\text{N}_2\text{O-N}_2$
734 values to calculate maximum and minimum estimates of $\% \text{B}_{\text{DEN}}$ (minimum, maximum and average
735 values adopted from Lewicka-Szczebak et al., (2016).

736 **Table 5** Ratios $\text{N}_2\text{O} / (\text{N}_2\text{O} + \text{N}_2)$ for all treatments

737 **Table 6** The temporal trends in $\delta^{15}\text{N}_{\text{bulk}}$, $\delta^{18}\text{O}$, $\delta^{15}\text{N}_{\text{a}}$, SP and $\% \text{B}_{\text{DEN}}$ for all experimental treatments

738 **Table 7** Equations of fitted functions and correlation coefficients corresponding to Figure 5 for Site
739 Preference vs $\delta^{18}\text{O}$ in all treatments for three periods.



740 References

741 Baggs, E.M., 2008. A review of stable isotope techniques for N₂O source partitioning in soils:
742 recent progress, remaining challenges and future considerations. *Rapid Commun. Mass Sp.*, 22,
743 1664-1672.

744 Baggs, E.M., Rees, R.M., Smith, K.A., Vinten, A.J.A., 2000. Nitrous oxide emission from soils
745 after incorporating crop residues. *Soil Use Manage.*, 16, 82-87.

746 Ball, B.C., Scott, A., Parker, J.P., 1999. Field N₂O, CO₂ and CH₄ fluxes in relation to tillage,
747 compaction and soil quality in Scotland. *Soil Till. Res.*, 53, 29-39.

748 Barré, P., Eglin, T., Christensen, B.T., Ciais, P., Houot, S., Kätterer, T., van Oort, F., Peylin, P.,
749 Poulton, P.R., Romanenkov, V., Chenu, C., 2010. Quantifying and isolating stable soil organic
750 carbon using long-term bare fallow experiments. *Biogeosciences*, 7, 3839-3850.

751 Bateman, E., Cadisch, G., Baggs, E., 2004. Soil water content as a factor that controls N₂O
752 production by denitrification and autotrophic and heterotrophic nitrification. *Controlling nitrogen*
753 *flows and losses. 12th Nitrogen Workshop, University of Exeter, UK, 21-24 September 2003*, 290-
754 292.

755 Bergstermann, A., Cardenas, L., Bol, R., Gilliam, L., Goulding, K., Meijide, A., Scholefield, D.,
756 Vallejo, A., Well, R., 2011. Effect of antecedent soil moisture conditions on emissions and
757 isotopologue distribution of N₂O during denitrification. *Soil Biol. Biochem.*, 43, 240-250.

758 Bol, R., Rockmann, T., Blackwell, M., Yamulki, S., 2004. Influence of flooding on delta N-15,
759 delta O-18, (1)delta N-15 and (2)delta N-15 signatures of N₂O released from estuarine soils - a
760 laboratory experiment using tidal flooding chambers. *Rapid Commun. Mass Sp.*, 18, 1561-1568.

761 Butterbach-Bahl, K., Baggs, E. M., Dannenmann, M., Kiese, R., Zechmeister-Boltenstern, S. 2013.
762 Nitrous oxide emissions from soils: how well do we understand the processes and their controls?
763 *Phil Trans R Soc B.*, 368: 20130122, <http://dx.doi.org/10.1098/rstb.2013.0122>.

764 Cardenas, L.M., Hawkins, J.M.B., Chadwick, D., Scholefield, D., 2003. Biogenic gas emissions
765 from soils measured using a new automated laboratory incubation system. *Soil Biol. Biochem.*, 35,
766 867-870.

767 Cardenas, L.M., Thorman, R., Ashlee, N., Butler, M., Chadwick, D., Chambers, B., Cuttle, S.,
768 Donovan, N., Kingston, H., Lane, S., Dhanoa, M.S., Scholefield, D., 2010. Quantifying annual N₂O
769 emission fluxes from grazed grassland under a range of inorganic fertiliser nitrogen inputs. *Agr.
770 Ecosyst. Environ.*, 136, 218-226.

771 Castellano, M.J., Schmidt, J.P., Kaye, J.P., Walker, C., Graham, C.B., Lin, H., Dell, C.J., 2010.
772 Hydrological and biogeochemical controls on the timing and magnitude of nitrous oxide flux across
773 an agricultural landscape. *Global Change Biol.*, 16, 2711-2720.

774 Clough, T.J., Muller, C., Laughlin, R.J., 2013. Using stable isotopes to follow excreta N dynamics
775 and N₂O emissions in animal production systems. *Animal : an international journal of animal
776 bioscience*, 7 Suppl 2, 418-426.

777 Cochran, W.G. and Cox, G.M., 1957. *Experimental Design*. John Wiley & Sons New York.

778 Crutzen, P.J., 1970. Influence of Nitrogen Oxides on Atmospheric Ozone Content. *Quarterly
779 Journal of the Royal Meteorological Society*, 96, 320.

780 Davidson, E.A., 1991. Fluxes of nitrous oxide and nitric oxide from terrestrial ecosystems. In:
781 Microbial production and consumption of greenhouse gases: Methane, nitrogen oxides and
782 halomethanes. J.E. Rogers and W.B. Whitman (eds.). American Society for Microbiology,
783 Washington, D.C., pp. 219-235.

784 Davidson, E.A., Hart, S.C., Shanks, C.A., Firestone, M.K., 1991. Measuring Gross Nitrogen
785 Mineralization, Immobilization, and Nitrification by N-15 Isotopic Pool Dilution in Intact Soil
786 Cores. *J. Soil Sci.*, 42, 335-349.

787 Davidson, E.A., Keller, M., Erickson, H.E., Verchot, L.V., Veldkamp, E., 2000. Testing a
788 conceptual model of soil emissions of nitrous and nitric oxides. *Bioscience*, 50, 667-680.

789 Davidson, E.A., Verchot, L.V., 2000. Testing the hole-in-the-pipe model of nitric and nitrous oxide
790 emissions from soils using the TRAGNET database. *Global Biogeochem. Cy.*, 14, 1035-1043.



791 Decock, C., Six, J., 2013. On the potential of delta O-18 and delta N-15 to assess N₂O reduction to
792 N₂ in soil. *Eur. J. Soil Sci.*, 64, 610-620.

793 del Prado, A., Merino, P., Estavillo, J.M., Pinto, M., Gonzalez-Murua, C., 2006. N₂O and NO
794 emissions from different N sources and under a range of soil water contents. *Nutr. Cycl. Agroecosys.*, 74, 229-243.

795 Deppe, M., Well, R., Giesemann, A., Spott, O., Flessa, H. 2017. Soil N₂O fluxes and related
796 processes in laboratory incubations simulating ammonium fertilizer depots. *Soil Biol. Biochem.*,
797 104, 68-80.

798 Dobbie, K.E., Smith, K.A., 2001. The effects of temperature, water-filled pore space and land use
799 on N₂O emissions from an imperfectly drained gleysol. *Eur. J. Soil Sci.*, 52, 667-673.

800 Firestone, M.K., Davidson, E.A., 1989. Microbiological basis of NO and N₂O production and
801 consumption in soil. *Exchange of Trace Gases between Terrestrial Ecosystems and the Atmosphere*,
802 47, 7-21.

803 Geisseler, D., Horwath, W.R., Joergensen, R.G., Ludwig, B., 2010. Pathways of nitrogen utilization
804 by soil microorganisms - A review. *Soil Biol. Biochem.*, 42, 2058-2067.

805 Gregory, A.S., Bird, N.R.A., Whalley, W.R., Matthews, G.P., Young, I.M., 2010. Deformation and
806 Shrinkage Effects on the Soil Water Release Characteristic. *Soil Sci. Soc. Am. J.*, 74, 4.

807 Harter, J., Guzman-Bustamente, I., Kuehfuss, S., Ruser, R., Well, R., Spott, O., Kappler, A.,
808 Behrens, S. 2016. Gas entrapment and microbial N₂O reduction reduce N₂O emissions from a
809 biochar-amended sandy clay loam soil. *Scientific Reports*, 6.

810 Hatch, D.J., Sprosen, M.S., Jarvis, S.C., Ledgard, S.F., 2002. Use of labelled nitrogen to measure
811 gross and net rates of mineralization and microbial activity in permanent pastures following
812 fertilizer applications at different time intervals. *Rapid Commun. Mass Sp.*, 16, 2172-2178.

813 IPCC, 2006. 2006 IPCC Guidelines for National Greenhouse Gas Inventories. 2006 IPCC
814 Guidelines for National Greenhouse Gas Inventories, Prepared by the National Greenhouse Gas
815 Inventories Programme, Eggleston H.S., Buendia L., Miwa K., Ngara T. and Tanabe K. (eds).
816 Published: IGES, Japan.

817 Klefth, R.R., Clough, T.J., Oenema, O., Groenigen, J.W., 2014a. Soil bulk density and moisture
818 content influence relative gas diffusivity and the reduction of nitrogen-15 nitrous oxide. *Vadose
819 Zone J.*, 13, 0089-0089.

820 Klefth, R.R., Clough, T.J., Oenema, O., Van Groenigen, J.-W., 2014b. Soil Bulk Density and
821 Moisture Content Influence Relative Gas Diffusivity and the Reduction of Nitrogen-15 Nitrous
822 Oxide. *Vadose Zone J.*, 13.

823 Koster, J.R., Cardenas, L.M., Bol, R., Lewicka-Szczebak, D., Senbayram, M., Well, R., Giesemann,
824 A., Dittert, K., 2015. Anaerobic digestates lower N₂O emissions compared to cattle slurry by
825 affecting rate and product stoichiometry of denitrification - An N₂O isotopomer case study. *Soil
826 Biol. Biochem.*, 84, 65-74.

827 Koster, J.R., Well, R., Dittert, K., Giesemann, A., Lewicka-Szczebak, D., Muhling, K.H.,
828 Herrmann, A., Lammel, J., Senbayram, M., 2013. Soil denitrification potential and its influence on
829 N₂O reduction and N₂O isotopomer ratios. *Rapid Commun. Mass Sp.*, 27, 2363-2373.

830 Kulkarni, M.V., Groffman, P.M., Yavitt, J.B., 2008. Solving the global nitrogen problem: it's a gas!
831 *Frontiers in Ecology and the Environment*, 6, 199-206.

832 Laudone, G.M., Matthews, G.P., Bird, N.R.A., Whalley, W.R., Cardenas, L.M., Gregory, A.S.,
833 2011. A model to predict the effects of soil structure on denitrification and N₂O emission. *J.
834 Hydrol.*, 409, 283-290.

835 Lewicka-Szczebak, D., Augustin J., Giesemann A., Well R., 2016a. Quantifying N₂O reduction to
836 N₂ based on N₂O isotopocules - validation with independent methods (Helium incubation and ¹⁵N
837 gas flux method). *Biogeosciences* (accepted manuscript).

838 Lewicka-Szczebak, D., Dyckmans, J., Kaiser, J., Marca, A., Augustin, J., Well, R., 2016b. Oxygen
839 isotope fractionation during N₂O production by soil denitrification. *Biogeosciences*, 13, 1129-1144.

840 Lewicka-Szczebak, D., Well, R., Bol, R., Gregory, A.S., Matthews, G.P., Misselbrook, T., Whalley,
841 W.R., Cardenas, L.M., 2015. Isotope fractionation factors controlling isotopocule signatures of soil-



843 emitted N₂O produced by denitrification processes of various rates. *Rapid Commun. Mass Sp.*, 29,
844 269-282.

845 Lewicka-Szczebak, D., Well, R., Koster, J.R., Fuss, R., Senbayram, M., Dittert, K., Flessa, H.,
846 2014. Experimental determinations of isotopic fractionation factors associated with N₂O production
847 and reduction during denitrification in soils. *Geochim. Cosmochim. Ac.*, 134, 55-73.

848 Liu, S.R., Herbst, M., Bol, R., Gottselig, N., Putz, T., Weymann, D., Wiekenkamp, I., Vereecken,
849 H., Bruggemann, N., 2016. The contribution of hydroxylamine content to spatial variability of N₂O
850 formation in soil of a Norway spruce forest. *Geochim. Cosmochim. Ac.*, 178, 76-86.

851 Ludwig, B., Bergstermann, A., Priesack, E., Flessa, H., 2011. Modelling of crop yields and N₂O
852 emissions from silty arable soils with differing tillage in two long-term experiments. *Soil Till. Res.*,
853 112, 114-121.

854 Mariotti, A., Germon, J.C., Leclerc, A., 1982. Nitrogen isotope fractionation associated with the
855 NO₂-- N₂O step of denitrification in soils. *Canadian J. Soil Sci.*, 62, 227-241.

856 Meijide, A., Cardenas, L.M., Bol, R., Bergstermann, A., Goulding, K., Well, R., Vallejo, A.,
857 Scholefield, D., 2010. Dual isotope and isotopomer measurements for the understanding of N₂O
858 production and consumption during denitrification in an arable soil. *Eur. J. Soil Sci.*, 61, 364-374.

859 Morley, N., Baggs, E.M., 2010. Carbon and oxygen controls on N₂O and N₂ production during
860 nitrate reduction. *Soil Biol. Biochem.*, 42, 1864-1871.

861 Mualem, Y., 1976. New model for predicting hydraulic conductivity of unsaturated porous-media.
862 *Water Resour. Res.*, 12, 513-522.

863 Muller, C. and Clough, T. J. 2014. Advances in understanding nitrogen flows and transformations:
864 gaps and research pathways. *J. Agric. Sci.*, 152: S34-S44.

865 Ostrom, N., Ostrom, P., 2011. The isotopomers of nitrous oxide: analytical considerations and
866 application to resolution of microbial production pathways. In: Baskaran M (ed). *Handbook*
867 *Environ Isot Geochem*. Springer: Berlin Heidelberg, 453-476.

868 Parton, W.J., Holland, E.A., Del Grosso, S.J., Hartman, M.D., Martin, R.E., Mosier, A.R., Ojima,
869 D.S., Schimel, D.S., 2001. Generalized model for NO_x and N₂O emissions from soils. *J. Geophys.*
870 *Res-Atmos.*, 106, 17403-17419.

871 Perez, T., Garcia-Montiel, D., Trumbore, S., Tyler, S., De Camargo, P., Moreira, M., Piccolo, M.,
872 Cerri, C., 2006. Nitrous oxide nitrification and denitrification N-15 enrichment factors from
873 Amazon forest soils. *Ecol. Appl.*, 16, 2153-2167.

874 Scheer, C., Wassmann, R., Butterbach-Bahl, K., Lamers, J.P.A., Martius, C., 2009. The relationship
875 between N₂O, NO, and N₂ fluxes from fertilized and irrigated dryland soils of the Aral Sea Basin,
876 Uzbekistan. *Plant Soil*, 314, 273-283.

877 Schmidt, U., Thoni, H., Kaupenjohann, M., 2000. Using a boundary line approach to analyze N₂O
878 flux data from agricultural soils. *Nutr. Cycl. Agroecosys.*, 57, 119-129.

879 Scholefield, D., Patto, P.M., Hall, D.M., 1985. Laboratory Research on the Compressibility of 4
880 Topsoils from Grassland. *Soil Till. Res.*, 6, 1-16.

881 Searle, P.L., 1984. The Berthelot or Indophenol Reaction and Its Use in the Analytical-Chemistry of
882 Nitrogen - a Review. *Analyst*, 109, 549-568.

883 Sutka, R.L., Ostrom, N.E., Ostrom, P.H., Breznak, J.A., Gandhi, H., Pitt, A.J., Li, F., 2006.
884 Distinguishing nitrous oxide production from nitrification and denitrification on the basis of
885 isotopomer abundances. *Appl. Environ. Microb.*, 72, 638-644.

886 Toyoda, S., Mutobe, H., Yamagishi, H., Yoshida, N., Tanji, Y., 2005. Fractionation of N₂O
887 isotopomers during production by denitrifier. *Soil Biol. Biochem.*, 37, 1535-1545.

888 Toyoda, S., Yoshida, N., 1999. Determination of nitrogen isotopomers of nitrous oxide on a
889 modified isotope ratio mass spectrometer. *Anal. Chem.*, 71, 4711-4718.

890 van der Weerden, T.J., Kelliher, F.M., de Klein, C.A.M., 2012. Influence of pore size distribution
891 and soil water content on nitrous oxide emissions. *Soil Research*, 50, 125-135.

892 van Genuchten, M.T., 1980. A closed form equation for predicting the hydraulic conductivity of
893 unsaturated soils. *Soil Sci. Soc. Am. J.*, 44, 892-898.



894 van Groenigen, J.W., Kuikman, P.J., de Groot, W.J.M., Velthof, G.L., 2005. Nitrous oxide emission
895 from urine-treated soil as influenced by urine composition and soil physical conditions. *Soil Biol.*
896 *Biochem.*, 37, 463-473.

897 Well, R., Augustin, J., Davis, J., Griffith, S.M., Meyer, K., Myrold, D.D., 2001. Production and
898 transport of denitrification gases in shallow ground water. *Nutr. Cycl. Agroecosys.*, 60, 65-75.

899 Well, R., Augustin, J., Meyer, K., Myrold, D.D., 2003. Comparison of field and laboratory
900 measurement of denitrification and N₂O production in the saturated zone of hydromorphic soils.
901 *Soil Biol. Biochem.*, 35, 783-799.

902 Well, R., Eschenbach, W., Flessa, H., von der Heide, C., Weymann, D., 2012. Are dual isotope and
903 isotopomer ratios of N₂O useful indicators for N₂O turnover during denitrification in nitrate-
904 contaminated aquifers? *Geochim. Cosmochim. Ac.*, 90, 265-282.

905 Well, R., Flessa, H., 2009. Isotopologue signatures of N₂O produced by denitrification in soils.
906 *J.Geophys. Res-Biogeogr.*, 114.

907 Well, R., Flessa, H., Xing, L., Ju, X.T., Romheld, V., 2008. Isotopologue ratios of N₂O emitted
908 from microcosms with NH₄⁺ fertilized arable soils under conditions favoring nitrification. *Soil Biol.*
909 *Biochem.*, 40, 2416-2426.

910 Well, R., Kurganova, I., de Gerenyu, V.L., Flessa, H., 2006. Isotopomer signatures of soil-emitted
911 N₂O under different moisture conditions - A microcosm study with arable loess soil. *Soil Biol.*
912 *Biochem.*, 38, 2923-2933.

913 Wu, D., Koster, J.R., Cardenas, L.M., Brüggemann, N., Lewicka-Szczebak, D., Bol, R., 2016. N₂O
914 source partitioning in soils using N-15 site preference values corrected for the N₂O reduction effect.
915 *Rapid Commun. Mass Sp.*, 30, 620-626.

916 Wu, D., Senbayram, M., Well, R., Brüggemann, N., Pfeiffer, B., Loick, N., Stempfhuber, B.,
917 Dittert, K., Bol, R. (2017) Nitrification inhibitors mitigate N₂O emissions more effectively under
918 straw-induced conditions favoring denitrification. *Soil Biol. Biochem.*, 104, 197-207.

919 Zhu, X., Burger, M., Doane, T.A., Horwath, W.R., 2013. Ammonia oxidation pathways and nitrifier
920 denitrification are significant sources of N₂O and NO under low oxygen availability. *P. Natl. Acad.*
921 *Sci. USA.*, 110, 6328-6333.

922 Zou, Y., Hirono, Y., Yanai, Y., Hattori, S., Toyoda, S., Yoshida, N., 2014. Isotopomer analysis of
923 nitrous oxide accumulated in soil cultivated with tea (*Camellia sinensis*) in Shizuoka, central Japan.
924 *Soil Biol. Biochem.*, 77, 276-291.

925

926

927



928 Table 1. Highfield soil properties
929

Property	Units	Highfield	930
			931
Location		Rothamsted Research	932
		Herts.	933
Grid reference	GB National Grid	TL129130	934
	Longitude	00°21'48"W	935
	Latitude	51°48'18"N	936
Soil type	SSEW ^a group ^c	Paleo-argillic brown earth	937
	SSEW ^a series ^d	Batcombe	938
	FAO ^{bc}	Chromic Luvisol	939
Landuse		Grass; unfertilised; cut	940
pH		5.63	941
Sand (2000-63 µm)	g g ⁻¹ dry soil	0.179	942
Silt (63-2 µm)	g g ⁻¹ dry soil	0.487	943
Clay (<2 µm)	g g ⁻¹ dry soil	0.333	944
Texture	SSEW ^a class ^c	Silty clay loam	945
Particle density	g cm ⁻³	2.436	946
Organic matter	g g ⁻¹ dry soil	0.089	947
Water content for packing	g g ⁻¹ dry soil	0.37	

948 ^aSoil Survey of England and Wales classification system

949 ^bUnited Nations Food and Agriculture Organisation World Reference Base for Soil Resources classification
950 system (approximation)

951 ^cAvery (1980)

952 ^dClayden & Hollis (1984)

953

954



955 Table 2. The four saturation conditions set for the Highfield soil.
956

Saturation condition	SAT/sat	HALFSAT/sat	UNSAT/sat	UNSAT/sat
Macropores	Saturated	Half-saturated	Unsaturated	Unsaturated
Micropores	Saturated	Saturated	Saturated	Half-saturated
<i>As prepared:</i>				
Matric potential, -kPa	4.1	12.3	27.3	136.9
Water content, g 100 g ⁻¹	47.7	42.5	37.2	29.4
Water content, cm ⁻³ 100 cm ⁻³	61.1	54.4	47.7	37.3
Water-filled pore space, %	98	91	82	68
Threshold pore size saturated, µm	73	24	11	2
<i>Final, following amendment:</i>				
Matric potential, -kPa	0	8.6	20.0	78.1
Water content, g 100 g ⁻¹	49.8	44.6	39.3	31.5
Water content, cm ⁻³ 100 cm ⁻³	63.8	57.1	50.4	40.0
Water-filled pore space, %	100	94	85	71
Threshold pore size saturated, µm	all	35	15	4

957
958
959



960
 961 Table 3. Contents of soil moisture, NO_3^- , NH_4^+ and C:N ratio and cumulative fluxes of N_2O and N_2 and CO_2 from all treatments at the end of the incubation. Values in
 962 brackets are standard deviation of the mean of three values.
 963

Treatment	% Mean moisture	NO_3^- , mg N kg^{-1} dry soil	NH_4^+ , mg N kg^{-1} dry soil	Total C, %	Total N, %	N_2O kg N ha^{-1}	N_2 kg N ha^{-1}	Total emitted N	CO_2 , kg C ha^{-1}
SAT/sat	39.8 (1.3)	1.1 (0.4)	104.3 (1.1)	3.61 (0.04)	0.35 (0.004)	9.4 (1.1)	54.0 (14.0)	63.4	289.2 (30.4)
HALFSAT/sat	40.2 (0.2)	0.8 (1.0)	104.2 (6.8)	3.64 (0.08)	0.36 (0.004)	10.9 (0.4)	51.7 (9.0)	62.6	283.0 (35.5)
UNSAT/sat	36.5 (2.1)	51.2 (37.4)	100.8 (5.7)	3.64 (0.10)	0.36 (0.007)	23.7 (11.0)	36.0 (28.5)	59.7	417.6 (57.1)
UNSAT/halfsat	34.3 (1.1)	100.6 (16.1)	71.3 (33.6)	3.53 (0.08)	0.36 (0.01)	16.8 (15.8)	17.2 (19.4)	34.1	399.7 (40.6)



966 Table 4: Scenarios with different combinations of $d^{18}\text{O}$ and Site Preference (SP) endmember values and $\eta_{\text{N}_2\text{O}}$
967 N_2 values to calculate maximum and minimum estimates of %Bden (minimum, maximum and average values
968 adopted from Lewicka-Szczabak et al., 2016a).
969

	SP0BD	SP0FDN	ηSP	$\eta^{18}\text{O}$
model (min endmember plus η)	-11	30	-2	-12
model (max endmember plus η)	0	37	-8	-12
model (max endmember)	0	37	-5.4	-12
model (min endmember)	-11	30	-5.4	-12
model (max η)	-5	33	-8	-12
model (min η)	-5	33	-2	-12

970
971
972



973 Table 5. Ratios $N_2O / (N_2O + N_2)$ for all treatments
974

Days	SAT/sat		HALFSAT/sat		UNSAT/halfsat		UNSAT/sat	
	mean	s.e.	mean	s.e.	mean	s.e.	mean	s.e.
-1	0.276	0.043	0.222	0.009	0.849	0.043	0.408	0.076
0	0.630	0.022	0.538	0.038	0.763	0.053	0.861	0.043
1	0.371	0.025	0.360	0.019	0.622	0.018	0.644	0.031
2	0.096	0.016	0.139	0.015	0.425	0.005	0.296	0.020
3	0.004	0.002	0.015	0.006	0.439	0.052	0.256	0.025
4	0.017	0.002	0.008	0.001	0.475	0.049	0.232	0.012
5	0.019	0.003	0.012	0.001	0.503	0.037	0.174	0.010
6	0.068	0.008	0.020	0.001	0.459	0.052	0.135	0.010
7	0.085	0.008	0.047	0.003	0.333	0.057	0.127	0.003
8	0.106	0.004	0.066	0.002	0.277	0.006	0.122	0.002
9	0.089	0.003	0.053	0.005	0.265	0.006	0.122	0.005
10	0.060	0.003	0.090	0.014	0.428	0.086	0.118	0.006
11	0.063	0.002	0.053	0.002	0.414	0.051	0.125	0.005

975
976



977 Table 6. The temporal trends in $\delta^{15}\text{N}_{\text{bulk}}$, $\delta^{18}\text{O}$, $\delta^{15}\text{N}_{\text{a}}$, Site Preference (SP) and %B_{DEN} for all experimental
 978 treatments (values in brackets are the standard deviation of the mean)

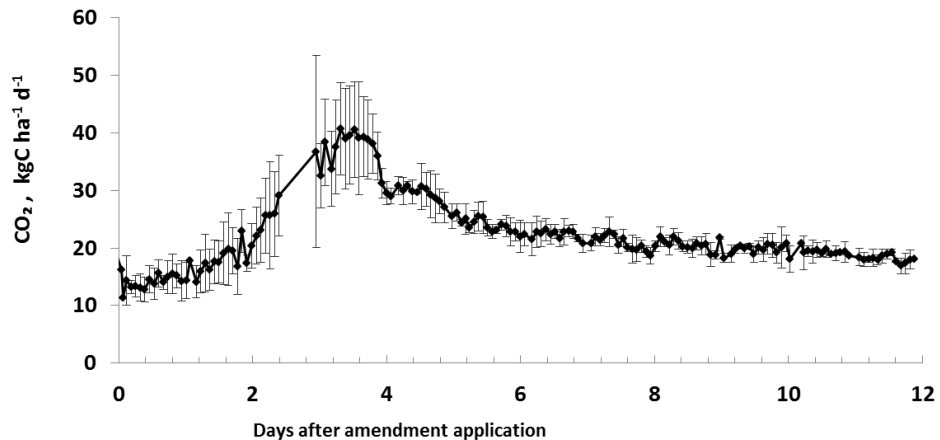
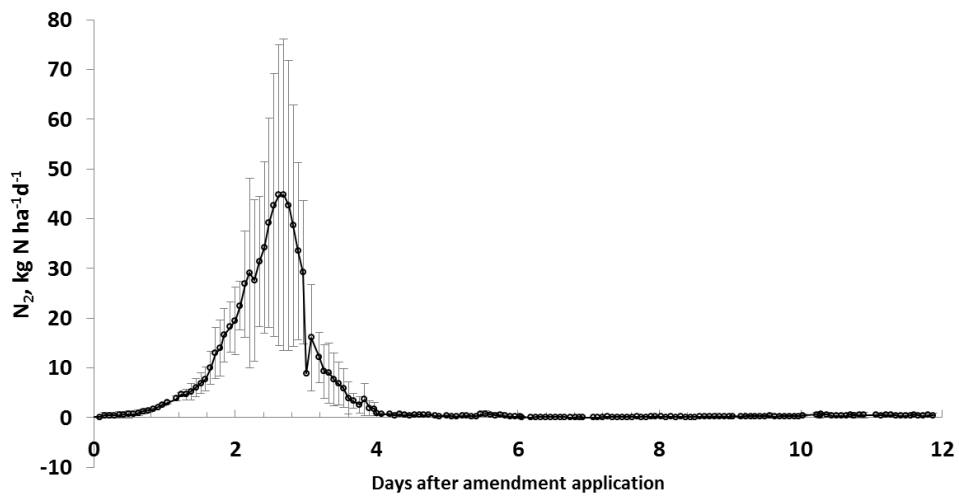
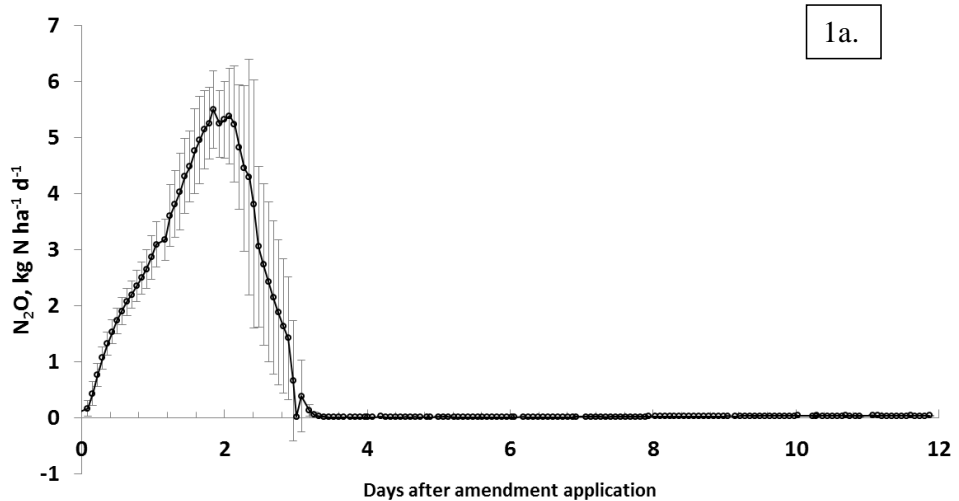
Day	$\delta^{15}\text{N}_{\text{bulkAIR}} (\text{\textperthousand})$			
	SAT/sat	HALFSAT/Sat	UNSAT/Sat	UNSAT/halfsat
-1	-3.8 (2.1)	-6.2 (1.5)	-14.2 (10.9)	-23.6 (1.1)
1	-18.9 (1.6)	-25.5 (4.6)	-20.3 (2.6)	-20.8 (2.3)
2	-7.7 (4.2)	-12.7 (2.7)	-12.2 (2.0)	-13.9 (5.7)
3	-2.4 (1.8)	14.0 (2.2)	-1.1 (7.6)	-4.4 (3.0)
4	-0.9 (2.2)	-0.3 (3.6)	-7.8 (4.6)	-9.3 (3.7)
5	-6.9 (0.9)	-4.3 (6.1)	-11.3 (3.7)	-8.9 (7.7)
7	-9.6 (1.5)	-10.0 (1.6)	-14.3 (4.7)	-13.4 (13.5)
12	-7.5 (1.2)	-8.6 (0.9)	-11.8 (2.6)	-21.3 (6.9)
$\delta^{18}\text{O}_{\text{SMOW}} (\text{\textperthousand})$				
	SAT/sat	HALFSAT/Sat	UNSAT/Sat	UNSAT/halfsat
-1	33.3 (2.6)	32.7 (3.0)	31.4 (9.8)	25.2 (4.9)
1	42.9 (2.4)	37.1 (3.8)	32.3 (3.6)	33.3 (2.1)
2	54.0 (5.7)	48.7 (4.5)	42.7 (5.3)	40.5 (5.0)
3	45.7 (1.5)	59.7 (3.2)	53.4 (5.7)	41.2 (1.0)
4	42.5 (1.4)	42.0 (3.7)	38.1 (4.5)	39.9 (7.7)
5	36.0 (2.9)	34.6 (3.7)	30.4 (2.6)	36.5 (6.9)
7	32.2 (5.5)	31.6 (5.5)	28.4 (4.4)	32.7 (5.4)
12	34.9 (5.6)	34.1 (2.7)	32.4 (2.9)	28.5 (5.0)
$\delta^{15}\text{N}_{\text{aAIR}} (\text{\textperthousand})$				
	SAT/sat	HALFSAT/Sat	UNSAT/Sat	UNSAT/halfsat
-1	-0.3 (3.4)	-2.6 (1.8)	-9.5 (12.0)	-19.7 (2.1)
1	-17.4 (1.8)	-24.0 (5.8)	-20.2 (2.0)	-21.1 (2.6)
2	-4.6 (4.2)	-9.5 (3.6)	-11.1 (1.1)	-13.8 (5.9)
3	-0.8 (1.3)	17.2 (4.0)	7.6 (4.7)	-2.7 (3.2)
4	1.0 (2.5)	0.7 (2.2)	-3.5 (3.7)	-2.8 (7.7)
5	-5.9 (0.7)	-2.9 (5.4)	-9.4 (3.9)	-5.2 (7.9)
7	-7.8 (2.3)	-5.3 (4.2)	-12.3 (5.6)	-7.7 (11.5)
12	-3.3 (2.1)	-4.6 (0.6)	-8.1 (4.2)	-15.3 (5.5)
SP _{AIR}				
	SAT/sat	HALFSAT/Sat	UNSAT/Sat	UNSAT/halfsat
-1	7.0 (3.9)	7.1 (4.2)	9.4 (2.1)	7.7 (1.9)
1	2.9 (0.6)	3.0 (2.3)	0.1 (1.8)	-0.7 (1.4)
2	6.3 (0.64)	6.4 (1.9)	2.2 (2.0)	0.2 (1.9)
3	3.3 (1.0)	6.4 (6.9)	11.9 (12.4)	5.9 (0.8)
4	3.7 (0.6)	2.0 (6.2)	8.7 (5.9)	5.4 (3.0)
5	2.0 (0.4)	3.0 (2.1)	3.9 (0.5)	7.4 (2.3)
7	5.0 (2.1)	9.2 (5.2)	3.9 (1.8)	11.2 (4.1)
12	8.4 (3.3)	7.9 (0.8)	7.3 (3.7)	11.8 (5.3)
Estimated range of %B _{DEN}				
	SAT/sat	HALFSAT/sat	UNSAT/sat	UNSAT/halfsat
-1	63-100	60-100	53-85	56-84
1-2	68-100	67-100	73-100	77-100
3-12	78-100	79-100	60-100	54-86

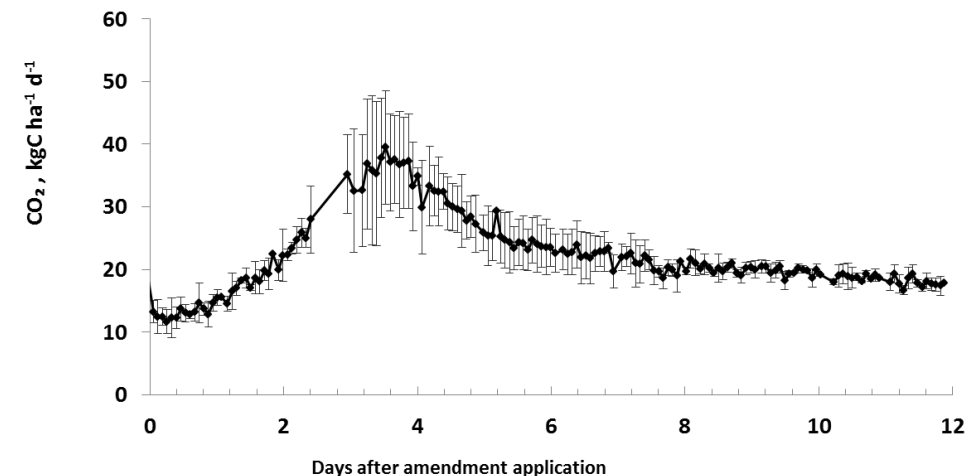
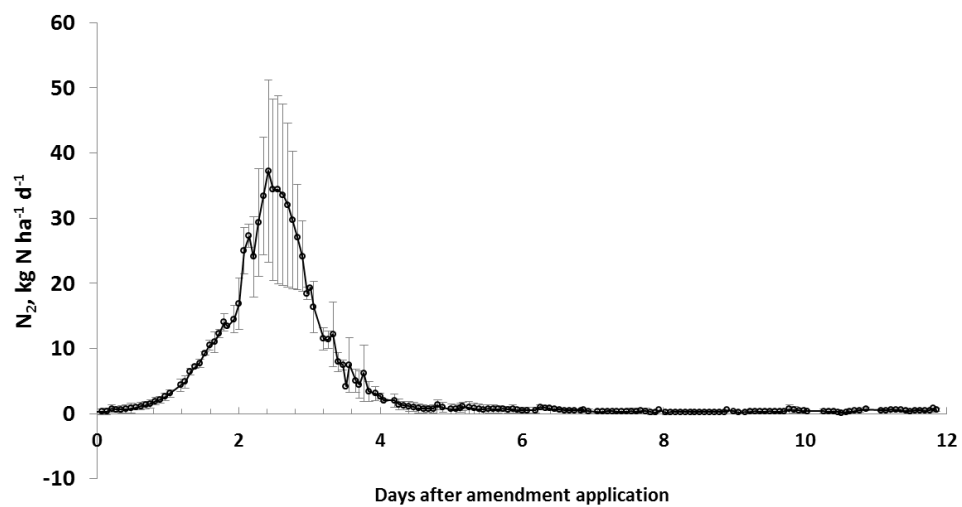
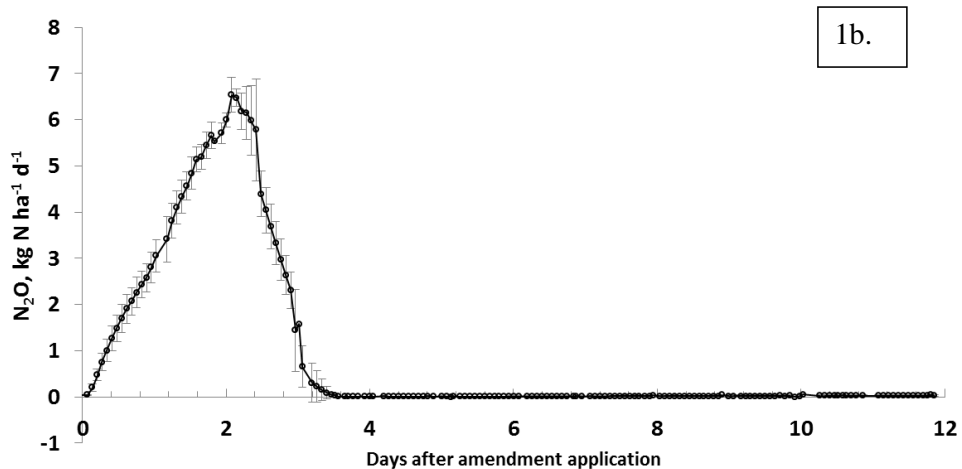


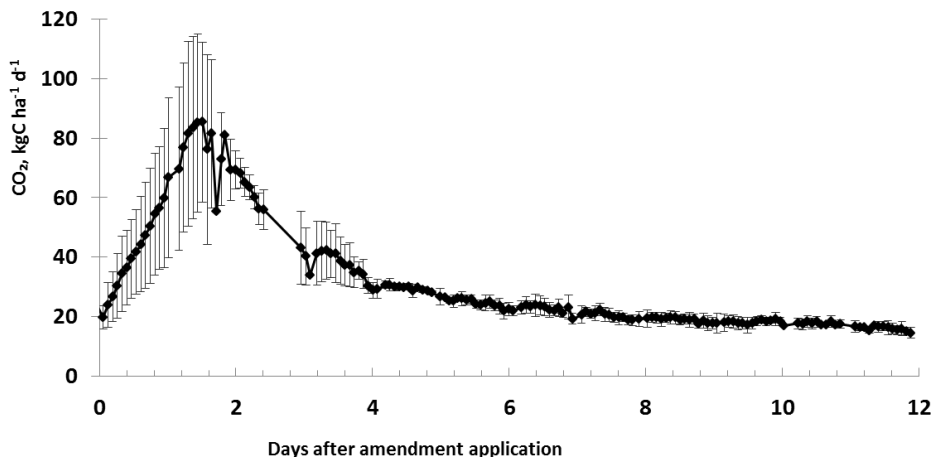
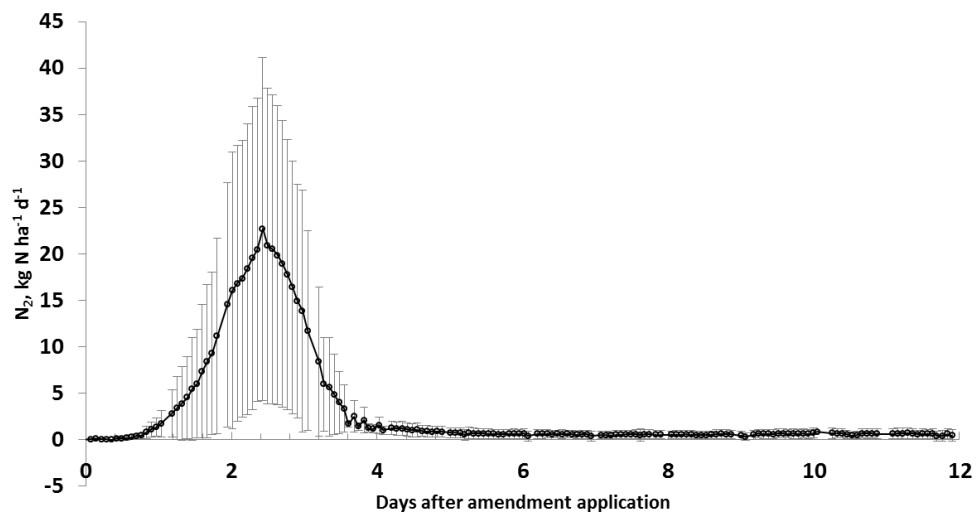
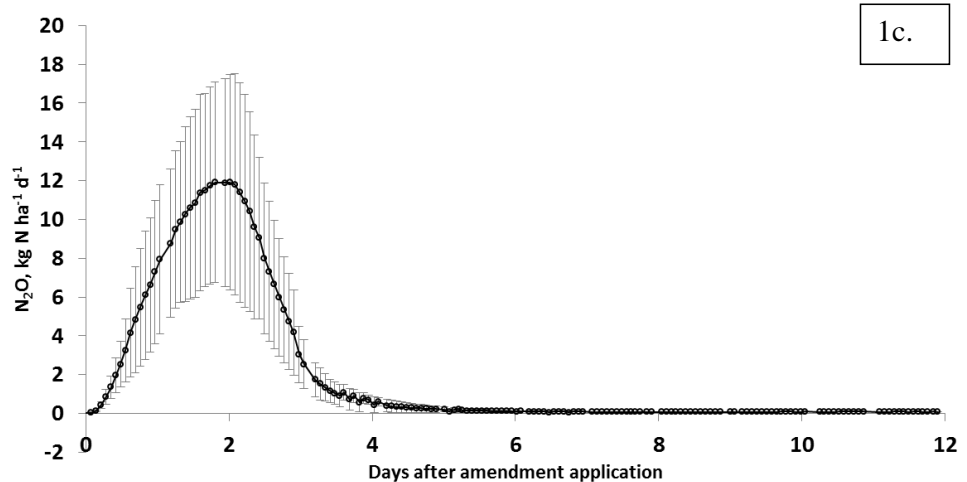
979 Table 7. Equations of fitted functions and correlation coefficients corresponding to Figure 5 for Site
980 Preference (SP) vs $\delta^{18}\text{O}$ in all treatments for three periods.
981

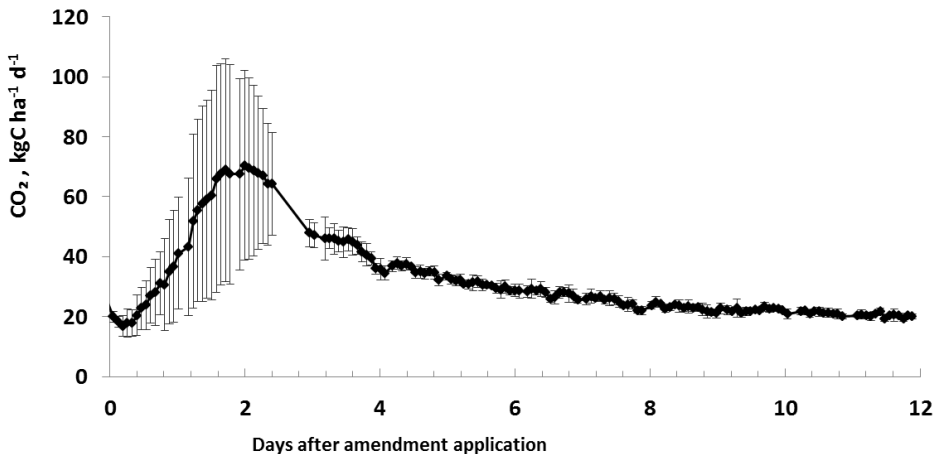
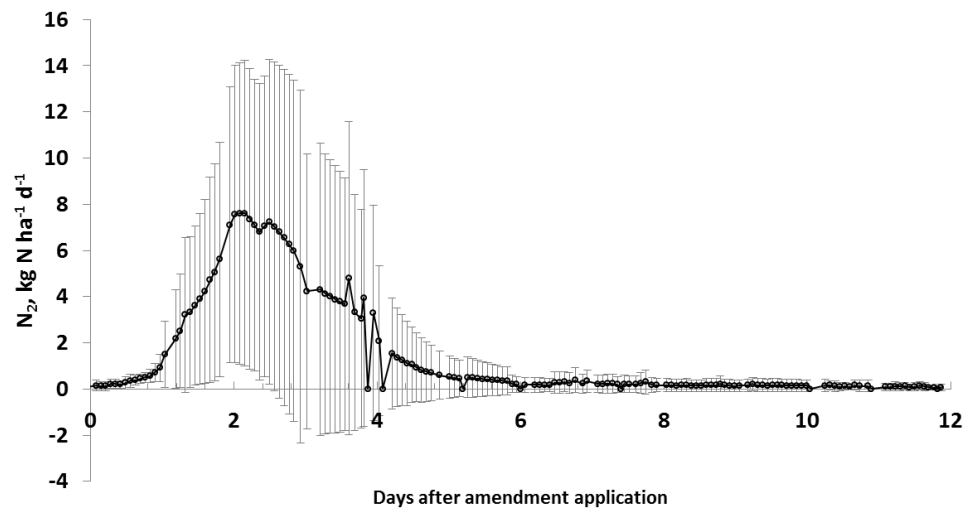
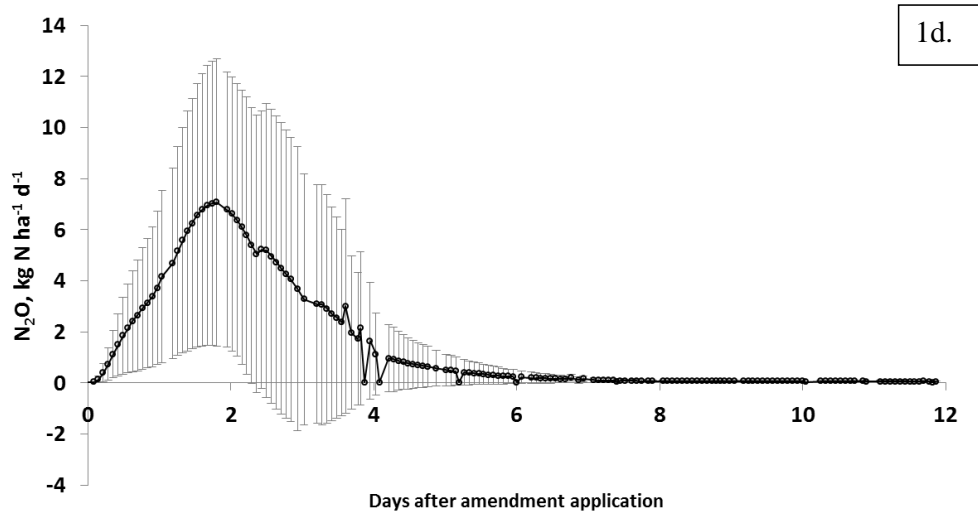
Treatment	Days 1-2	Days 3-5	Days 7-12
SAT/sat	$y = 0.2151x - 5.8386, R^2 = 0.6529$	$y = 0.1204x - 1.848, R^2 = 0.397$	$y = 0.5872x - 12.223, R^2 = 0.985$
HALFSAT/sat	$y = 0.3447x - 10.129, R^2 = 0.9048$	$y = 0.23x - 7.0689, R^2 = 0.2188$	$y = 0.4063x - 6.2632, R^2 = 0.6876$
UNSAT/sat	$y = 0.2709x - 8.9968, R^2 = 0.8664$	$y = 0.7248x - 18.874, R^2 = 0.507$	$y = 0.6848x - 15.236, R^2 = 0.7156$
UNSAT/halfsat	$y = -0.0146x + 0.2506, R^2 = 0.0024$	$y = 0.3589x - 7.2194, R^2 = 0.4839$	$y = -0.318x + 21.261, R^2 = 0.1491$

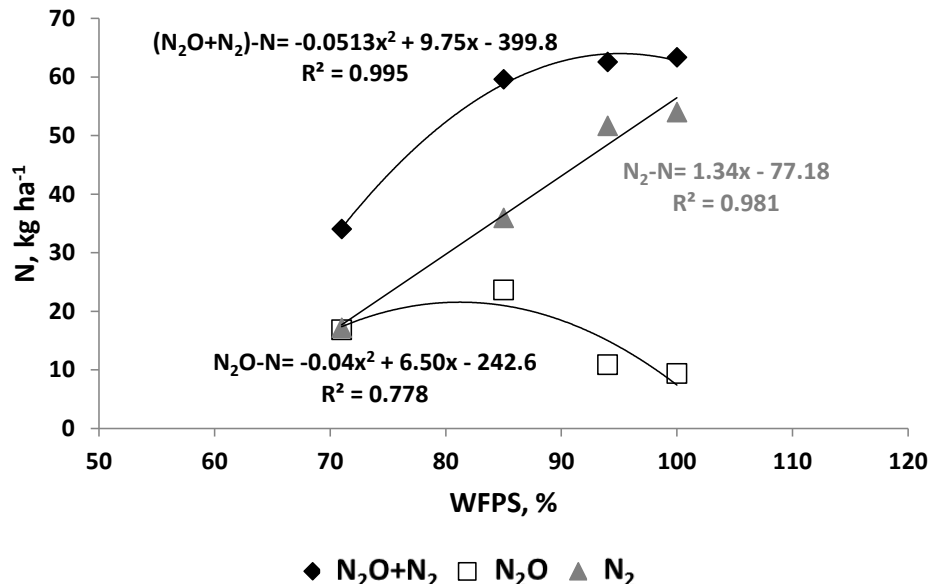
982
983



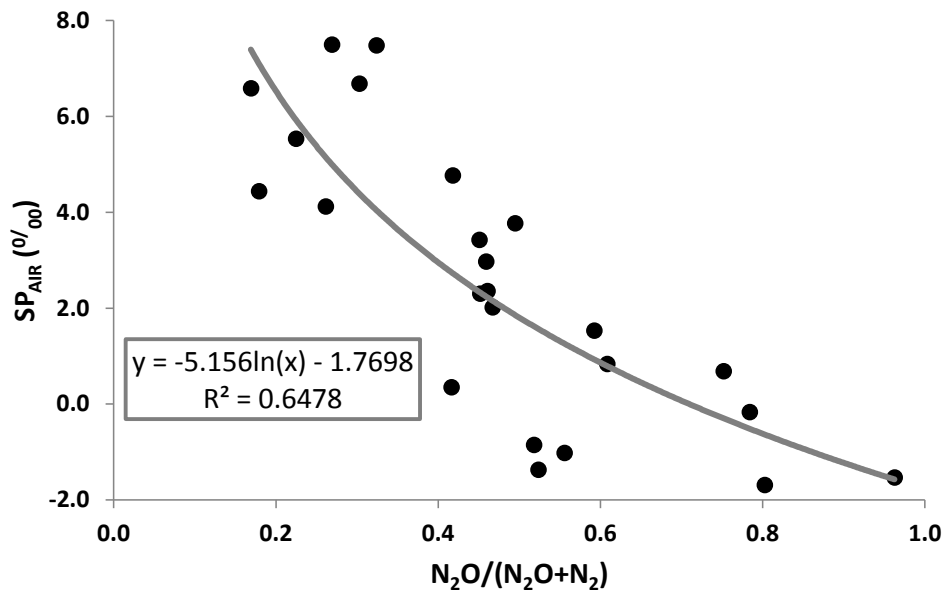




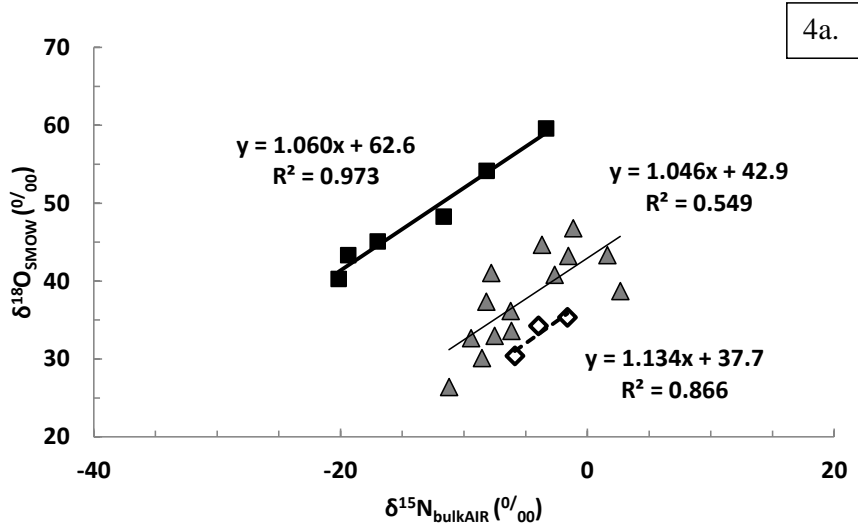




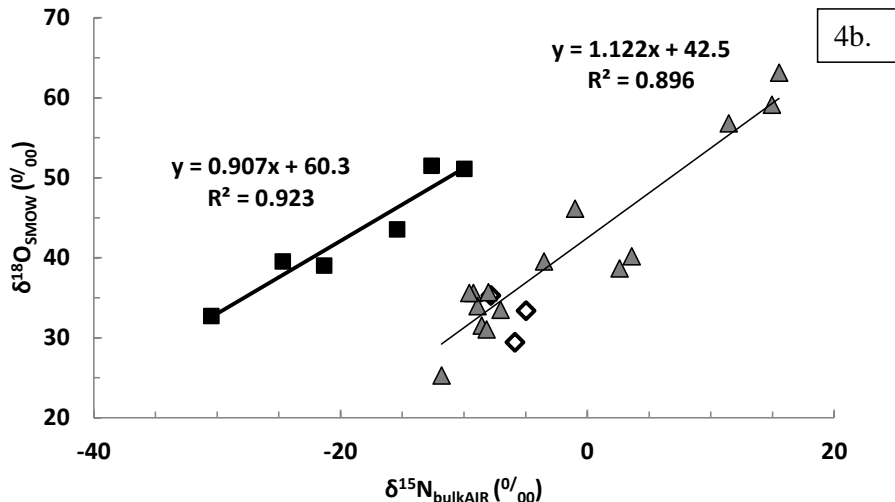
988
989 Figure 2
990
991



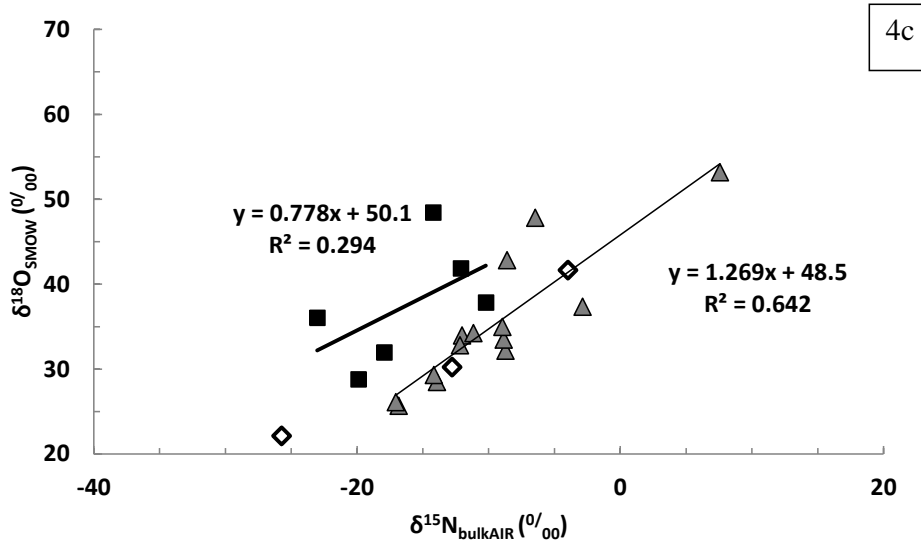
992
993 Figure 3
994
995



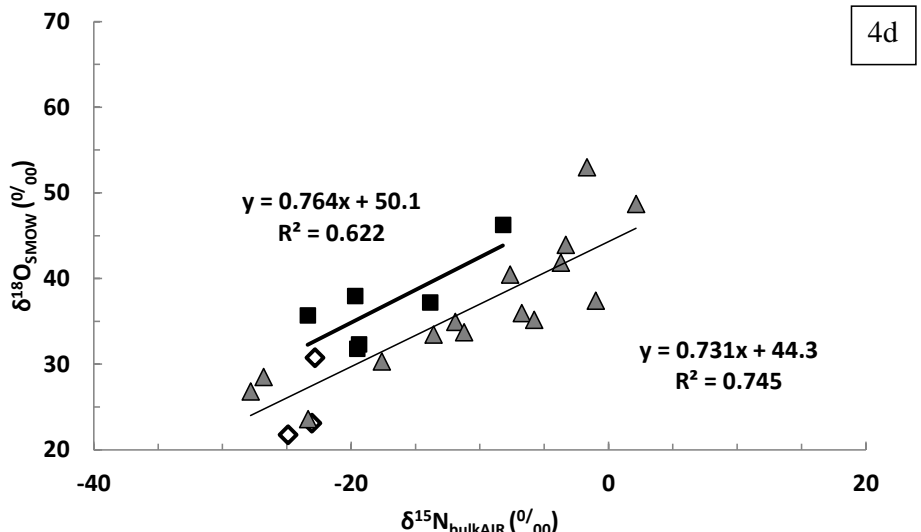
996
997
998
999



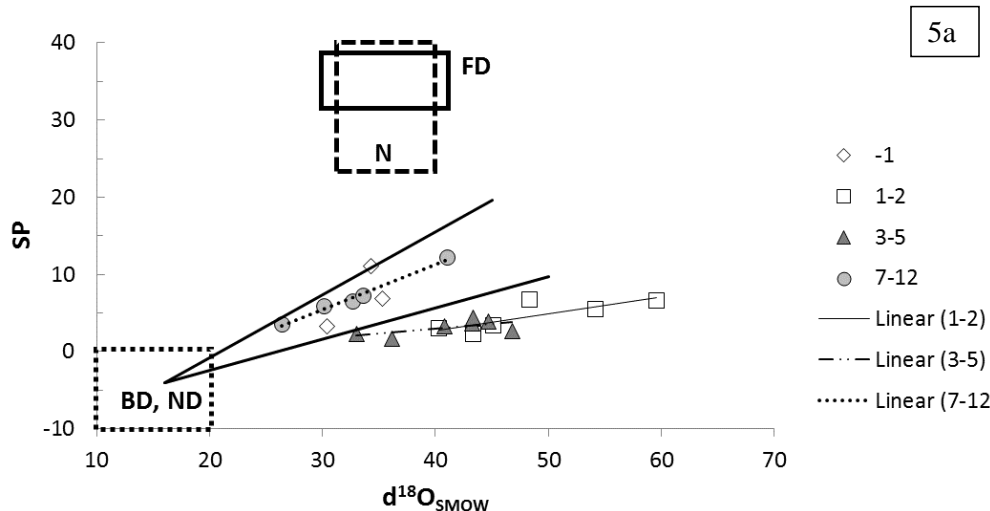
1000
1001



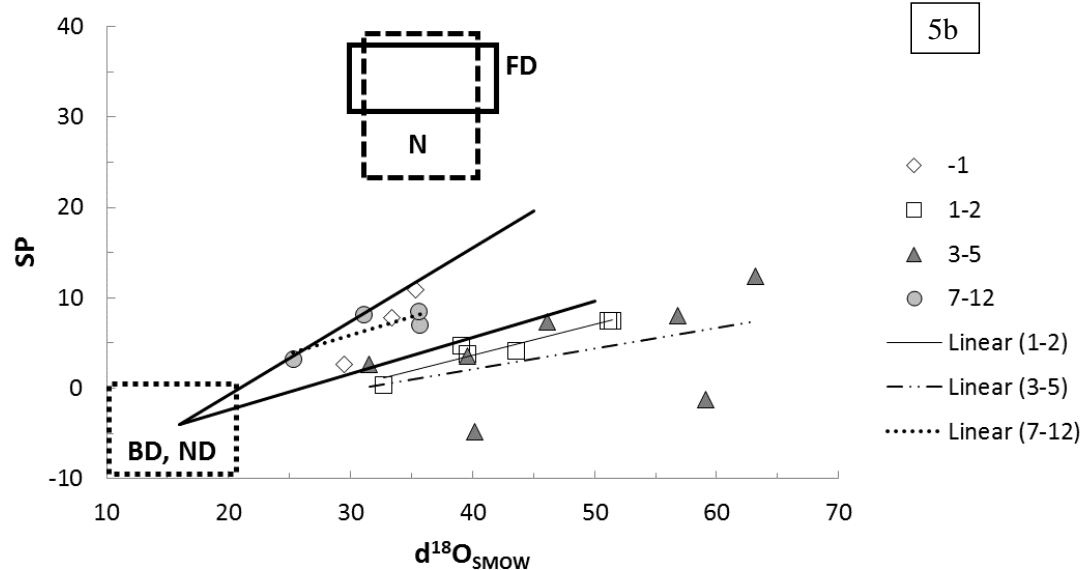
1002
 1003
 1004



1005
 1006
 1007



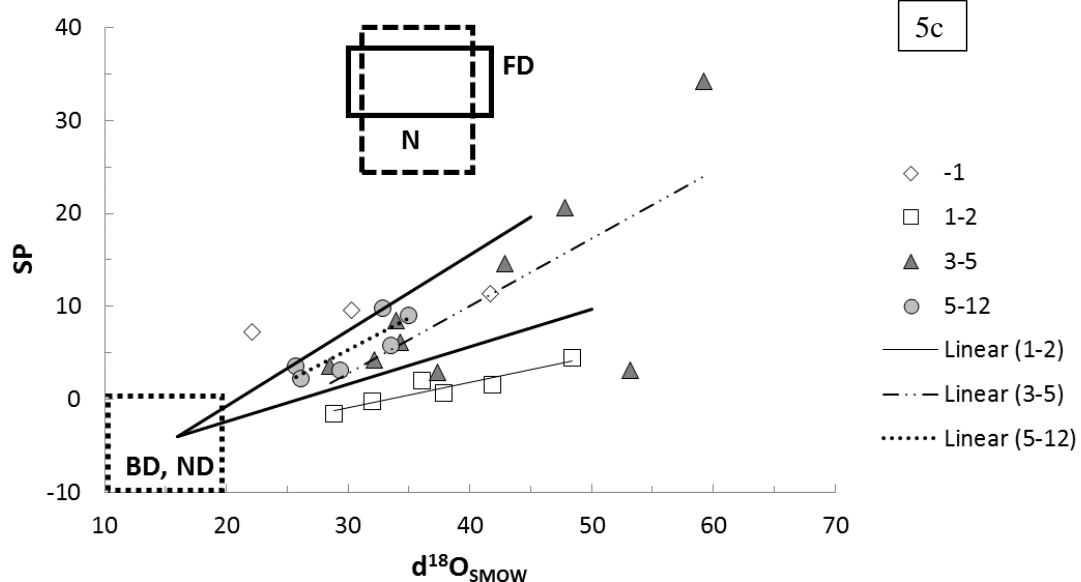
1008
 1009
 1010



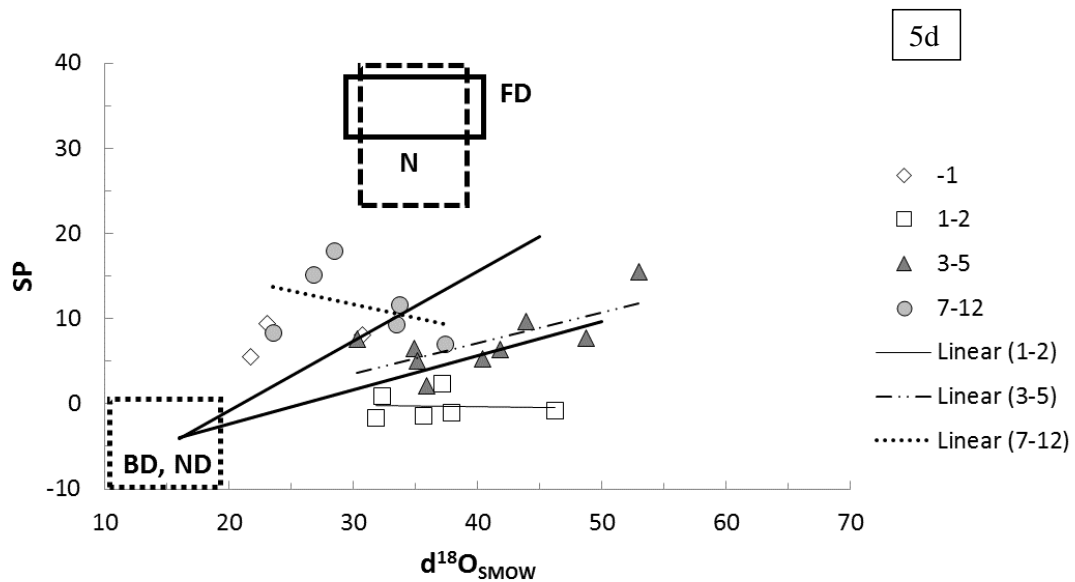
1011
 1012
 1013
 1014
 1015
 1016
 1017
 1018
 1019



1020



1021
 1022
 1023



1024